Article:

Gokul, J.K., Hodson, A.J., Saetnan, E.R. et al. (7 more authors) (2016) Taxon interactions control the distributions of cryoconite bacteria colonizing a High Arctic ice cap. Molecular Ecology, 25 (15). pp. 3752-3767. ISSN 0962-1083

https://doi.org/10.1111/mec.13715

This is the peer reviewed version of the following article: Gokul, J.K., Hodson, A.J., Saetnan, E.R., Irvine-Fynn, T.D., Westall, P.J., Detheridge, A.P., Takeuchi, N., Bussell, J., Mur, L.A. and Edwards, A. (2016) Taxon interactions control the distributions of cryoconite bacteria colonizing a High Arctic ice cap. Molecular Ecology., which has been published in final form at http://dx.doi.org/10.1111/mec.13715. This article may be used for non-commercial purposes in accordance with Wiley Terms and Conditions for Self-Archiving (http://olabout.wiley.com/WileyCDA/Section/id-828039.html)

Taxon interactions control the distributions of cryoconite bacteria colonizing a High Arctic ice cap

Journal:	*Molecular Ecology*
Manuscript ID	MEC-15-1529.R1
Manuscript Type:	Original Article
Date Submitted by the Author:	n/a
Complete List of Authors:	Gokul, Jarishma; Aberystwyth University, Institute of Biological, Environmental & Rural Sciences Hodson, Andrew; University of Sheffield, Geography; Universitetssenteret pa Svalbard AS, Arctic Geology Saetnan, Eli; Aberystwyth University, Institute of Biological, Environmental & Rural Sciences Irvine-Fynn, Tristram; Aberystwyth University, Geography and Earth Sciences Westall, Phillipa; Aberystwyth University, Institute of Biological, Environmental and Rural Sciences Detheridge, Andrew; Aberystwyth University, Institute of Biological, Environmental and Rural Sciences Takeuchi, Nozomu; Chiba University, Department of Earth Sciences Bussell, Jennifer; University of Nottingham Mur, Luis; Aberystwyth University, Institute of Biological, Environmental and Rural Sciences Edwards, Arwyn; Aberystwyth University, IBERS
Keywords:	Svalbard, cryoconite, biogeography, ecosystem engineering, keystone species, Bacteria

Taxon interactions control the distributions of cryoconite bacteria colonizing a High Arctic ice cap

Jarishma K. Gokul[1], Andrew J. Hodson[2,3], Eli R. Saetnan[1], Tristram D.L., Irvine-Fynn[4], Philippa J. Westall[1], Andrew P. Detheridge[1], Nozomu Takeuchi[5], Jennifer Bussell[1,6] Luis A.J. Mur[1], Arwyn Edwards*[1].

Postal Address: [1]Institute of Biological, Rural and Environmental Sciences, Cledwyn Building, Aberystwyth University, Aberystwyth, UK. [2]Department of Geography, University of Sheffield, Sheffield, UK. [3]Department of Arctic Geology, University Centre in Svalbard (UNIS), Longyearbyen, Svalbard. [4]Department of Geography and Earth Sciences, Aberystwyth University, Llandinam Building, Aberystwyth, UK. [5]Department of Earth Sciences, Graduate School of Science, Chiba University, 1-33, Yayoicho, Inage-ku, Chiba, Japan. [6]University of Nottingham, Sutton Bonington Campus, Loughborough, Leicestershire, LE12 5RD.

Keywords: Svalbard / Cryoconite / biogeography / ecosystem engineering / keystone species / bacteria

*Corresponding Author: Arwyn Edwards, Institute of Biological, Rural and Environmental Sciences, Aberystwyth University, Aberystwyth, UK aye@aber.ac.uk

Running title: Bacterial biogeography of a High Arctic ice cap.

Abstract (247 words)

Microbial colonization of glacial ice surfaces incurs feedbacks which affect the melting rate of the ice surface. Ecosystems formed as microbe-mineral aggregates termed cryoconite locally reduce ice surface albedo and represent foci of biodiversity and biogeochemical cycling. Consequently, greater understanding the ecological processes in the formation of functional cryoconite ecosystems upon glacier surfaces is sought. Here we present the first bacterial biogeography of an ice cap, evaluating the respective roles of dispersal, environmental and biotic filtration occurring at local scales in the assembly of cryoconite microbiota. 16S rRNA gene amplicon semiconductor sequencing of cryoconite colonizing a Svalbard ice cap coupled with digital elevation modelling of physical parameters reveals the bacterial community is dominated by a ubiquitous core of generalist taxa, with evidence for a moderate pairwise distance-decay relationship. While geographic position and melt season duration are prominent among environmental predictors of community structure, the core population of taxa appears highly influential in structuring the bacterial community. Taxon co-occurrence network analysis reveals a highly modular community structured by positive interactions with bottleneck taxa, predominantly *Actinobacteria* affiliated to isolates from soil humus. In contrast, the filamentous cyanobacterial taxon (assigned to *Leptolyngbya*) which dominates the community and bind together granular cryoconite are poorly connected to other taxa. While our study targeted one ice cap, the prominent role of generalist core taxa with close environmental relatives across the global cryosphere indicate discrete roles for cosmopolitan *Actinobacteria* and *Cyanobacteria* as respective keystone taxa and ecosystem engineers of cryoconite ecosystems colonizing ice caps.

INTRODUCTION

The interactions of glacial systems with climate, water and landscape assume considerable scientific and societal concern. This interest pre-dates the appreciation that glaciers, ice caps and ice sheets comprise microbial ecosystems (Hodson *et al.* 2008). Indeed, the activities of biodiverse microbial ecosystems associated with glacial habitats interact with both the dynamics of glacial systems and influence biogeochemical cycles (Edwards *et al.* 2014a; Hood *et al.* 2015; Rime *et al.* 2015). At the glacier surface, cryoconite ecosystems are recognized as major foci of microbial biodiversity and activity (Cameron *et al.* 2012; Cook *et al.* 2015b; Edwards *et al.* 2011) which influence ice surface albedo (Bøggild 1997; Takeuchi 2002) and potentially ice topography (Cook *et al.* 2015a).

The darkening action of granular microbe-mineral aggregates, termed cryoconite, upon ice surfaces causes localized melting and so cryoconite ecosystems often occupy quasi-circular holes within the ice surface which interact with the hydrology of the porous ice surface (Cook *et al.* 2015c; Edwards *et al.* 2011). The cryoconite biota includes viruses, bacteria, fungi, other micro-eukaryotes and meiofauna (Säwström *et al.* 2002) which actively contribute to carbon and nitrogen cycling (Hodson *et al.* 2007l; Segawa *et al.* 2014). On both Arctic and alpine glaciers, the composition and structure of cryoconite bacterial communities are closely related to the rates of microbial activities and the composition of cryoconite organic matter (Edwards *et al.* 2011; Edwards *et al.* 2014b; Edwards *et al.* 2013a). It appears that filamentous cyanobacteria (e.g. *Phormidium, Phormidesmis* or *Leptolyngbya* sp.) aggregate aeolian debris (Hodson *et al.* 2010; Langford *et al.* 2010), engineering the formation of granular cryoconite forming microbial communities distinctive from proximal habitats (Edwards *et al.* 2013b; Musilova *et al.* 2015). While the role of filamentous cyanobacteria is pivotal to the formation of stable cryoconite granules (Langford *et al.* 2010) harbouring a diverse community of bacterial heterotrophs, whether cyanobacteria represent keystone species or ecosystem engineers is equivocal (Edwards *et al.* 2014b). Similarly, while commonly-occurring taxa in a given habitat, termed the core taxa, are assumed to regulate ecosystem functioning, and rare taxa (present within the long tail of a taxon abundance curve) may represent a store of genomic and functional variability as a "seed bank" (Fuhrman 2009, whether core and tail taxa in cryoconite bacterial communities occur as generalists and specialists with broad- and narrow- shaped niches respectively{Barberan, 2012 #833; Pedrós-Alió 2006) is poorly defined. Understanding the topology of the network of interactions between taxa varying in abundance and ubiquity (Barberan *et al.* 2012; Peura *et al.* 2015; Steele *et al.* 2011) can therefore be expected to enhance our understanding of how cryoconite bacterial communities colonize ice surfaces, accumulating organic matter and accelerating ice melt (Cook *et al.* 2015a; Cook *et al.* 2015b).

Moreover, while previous studies have shown clear evidence of inter-regional and inter-glacier differences in cryoconite bacterial communities (Cameron *et al.* 2012; Edwards *et al.* 2011) the drivers and extent of spatial variation within the scale of individual glaciers are unclear. Recently, Langford *et al.* (2014) conducted a high-resolution sampling of cryoconite properties on a single Svalbard valley glacier, finding only moderate evidence for changes in the properties of cryoconite granules across the ice surface. Likewise Edwards *et al.* (2011) reported that inter-glacier differences outweighed very weak distance-decay relationships in bacterial community structure on three Svalbard valley glaciers. Furthermore, the temporal dynamics of cryoconite bacterial communities are less clear, with contrasting inferences made from intra-seasonal sampling of cryoconite ecosystems at the margin of Greenland's ice sheet in two recent studies (Musilova *et al.* 2015; Stibal *et al.* 2015).

Consequently, the influence of seasonal melting upon community history or the response of cryoconite bacterial communities to environmental drivers prevailing within stable, low-gradient ice masses is unknown. This is likely to be the consequence of truncated environmental gradients associated with a low-complexity landscape responding to melt-associated drivers over a short dynamic range as the melting season proceeds rapidly. While studies of species turnover across elongated environmental gradients, for example at the ice sheet scale, could provide further insights, these will be across a broader, potentially continental, biogeographical scale since ice sheets span latitudinal and climatological gradients.

In contrast, ice caps provide an attractive model system for exploring the biogeography of microbial community development. Ice caps are defined as terrestrial ice masses which are not constrained by the topography of their underlying terrain but rather are shaped principally by their surface mass balance, and as distinct from ice sheets, have a surface area of less than 50,000 km^2 (Benn & Evans 2014). Consequently, by virtue of their surface topography, ice-cap associated microbial communities are likely to be situated within strong local environmental gradients within the same locality. Therefore, we hypothesize that the relative influence of dispersal, environmental and biotic filters in the assembly of cryoconite bacterial communities can be evaluated by respectively examining distance-decay relationships, linkages with physical parameters and taxon interactions of ice cap cryoconite microbiota.

In this study, we collected cryoconite from across an entire ice cap in the High Arctic archipelago of Svalbard which was constrained by a high resolution digital elevation model, permitting a detailed analysis of the bacterial biogeography in relation to the topography of the ice cap. We show that geographic position and melt season duration do influence community structure, with evidence of a moderate distance-decay relationship in community

similarity and the dominance of a core population comprising generalist taxa. Co-occurrence network analysis based identification of keystone species among heterotrophic bacteria rather than filamentous cyanobacteria which are considered ecosystem engineers. We conclude that biotic filtering (i.e. taxon-taxon interactions such as competition or cooperation) plays a critical but hitherto unrecognized role in the microbial colonization of ice surfaces.

MATERIALS AND METHODS

Site description and Sampling

Foxfonna is an ice cap measuring approximately 4 km^2 in central Svalbard (78˚ 08'N, 16˚ 07' E; Figure 1) with ice elevations ranging from ~675 to 955 m a.s.l (Rutter *et al.* 2011). The ice cap dome is almost decoupled from two small outlet glaciers descending to 285 m a.s.l.: Rieperbreen to the west and an unnamed outlet glacier to the north. Typically, the ice cap dome experiences melt for a short (~45 day) period of the summer. Surface mass balance measurements at seven stakes drilled into the ice cap indicate an average net annual balance of -0.25 +/- 0.36 (s.d.) m water equivalent for the period 2007 – 2014 (Rutter *et al.*, (2011);. The strong variability is caused by occasional positive balance years for the ice cap, which last occurred during 2008 and 2012. Cryoconite samples were collected from the dome-shaped higher elevations (>700 m a.s.l.) of the ice cap on the 23rd of August 2011, towards the end of an ablation season during what was a close to average net mass balance year at the site (i.e. -0.38 m water equivalent). As is common at elevations proximate to the late summer snow line in Svalbard (Wadham *et al.* 2006) the superimposed ice layer was decaying and facilitated the development and exposure of cryoconite debris. Sampling was undertaken at four sectors according to aspect (hereafter G1, G2, G3, G4) over the ice cap surface. At 37 locations across the ice cap, cryoconite debris was aspirated into sterile 15 mL tubes and transferred on ice to -80°C frozen storage within four hours for three weeks and thereafter transferred frozen in insulated containers within ten hours, to -80°C storage in the UK. The surface area cover of cryoconite, termed, Apparent Cryoconite Area (ACA) was calculated as previously detailed (Irvine-Fynn *et al.* 2010) while chlorophyll a was quantified from cryoconite slurries as described (Langford *et al.* 2014).

Digital Elevation Model

Elevation data coupled with high-resolution aerial imagery was used to compile a digital elevation model (DEM) of the ice cap surface with a 5 m horizontal resolution. Due to the likely presence of noise in the raw elevation data, a standard smoothing filter was applied to the DEM (Wise 2000).

Primary (e.g. slope, aspect) and secondary (e.g. curvature, hydrological flow) indices were extracted from the smoothed DEM using ESRI's ArcGIS software. The indices describing the ice cap surface character and topographic attributes were retrieved using the ArcGIS "Spatial Analyst" tool-set following established recommendations (e.g. (Moore *et al.* 1991). While both slope and aspect dictate solar radiation receipt at the ice surface, slope also serves as a proxy for local meltwater flow velocity and an index for potential hydrological disturbance. Rather than using slope as a proxy for meltwater discharge, the Flow Accumulation Area (hereafter, FAA) defined as the upslope area in m^2 draining to location point was used to represent a meltwater discharge regime. With knowledge that meltwater flow on Arctic glacier surfaces occurs dominantly through a near-surface perched aquifer (Irvine-Fynn & Edwards 2013; Irvine-Fynn *et al.* 2011), the topographic wetness index as a function of FAA and slope provides a continuous descriptor for areas over the ice cap likely considered to range between well-drained or water-saturated. The convex nature of the ice cap surface rendered use of the d8 algorithm (Jenson & Domingue) more appropriate than alternatives (e.g. Tarboton (1997)) for prescribing flow routing over the ice cap surface.

Additional indices describing the surface conditions were calculated from the DEM. Potential incident radiation (IR) receipt for all locations across the ice cap throughout the summer melt season in 2011 was calculated following standard algorithms (Irvine-Fynn *et al.* 2014). Local variability in cloud cover precluded accurate, distributed estimations of actual radiation receipt at each sample site. However, spatially distributed air temperature records were extrapolated from data collected at the weather station on the outlet glacier to the north of Foxfonna (Figure 1) using a local air temperature lapse rate of -0.65 °C per 100 m elevation. Measures of melt intensity in the form of a count of hours > 0°C (PositiveHrs), positive degree days (PDDs) and positive degree hours (PDHrs; see (Hock 2005))were derived from the extrapolated weather station record.

This range of environmental parameters were extracted from the DEM for each sample site and normalized in Primer6/PERMANOVA+ (PRIMER-E Ltd) for use with multivariate analyses.

Sample handling and DNA Extraction

All samples were handled in a bleach-decontaminated laminar flow hood using sterile tools and certified DNA free plasticware as previously detailed (Edwards *et al.* 2011). Negative extraction and PCR controls were included to verify the absence of contamination based upon the absence of a band upon gel electrophoresis, but not sequenced. Community genomic DNA was extracted from 0.5g of wet cryoconite using a CTAB/Phenol - chloroform bead-beating based extraction and polyethylene glycol precipitation (Griffiths *et al.* 2000) as previously described (Hill *et al.* 2015) and detailed in supplementary methods. Reagents were DEPC-treated and autoclaved. DNA quality checks by agarose gel and preliminary 16S rRNA gene T-RFLP were performed as described previously (Edwards *et al.* 2014b) and extraction and negative template controls did not yield product.

16S ribosomal RNA gene amplicon semiconductor sequencing

Bacterial 16S rRNA gene regions were PCR amplified using barcoded V1 and V3 primers (B-27F + MID; A1-357R; supplementary table 1) in a single batch prior to semiconductor sequencing on a single Ion Torrent 316v2 chip exactly as described (Hill *et al.* 2015) and supplementary methods. Amplification, library preparation and sequencing were conducted in a single batch. Sequence data are available at EBI-SRA (SRP067436 : PRJNA306097).

Sequence processing and bioinformatics

Resulting sequences were quality filtered in Python using Mothur (Schloss *et al.* 2009) with the USEARCH algorithm (Edgar 2010) before performing closed-reference OTU picking in QIIME 1.9.0 (Caporaso *et al.* 2010) using the Greengenes 13_8 reference database (DeSantis *et al.* 2006). OTUs were clustered at a threshold of 97% and sequence taxa assignments and chimera checking were performed in QIIME using uclust (Edgar 2010) and RDP classifier version 2.2 (Wang *et al.* 2007). Permutational Multivariate Analysis of Variance (PERMANOVA), Canonical Analysis of Principal Components (CAP), distance-based linear modelling (distLM), were performed with fourth-root transforms of Bray Curtis distances based upon OTU relative abundance, while the Mantel-based test RELATE was performed with 999 permutations using a resemblance matrix of the fourth-root transformed Bray-Curtis distances and pairwise physical distances. Default options were selected for CAP, including performance of leave-one-out analyses, an iterative cross-validation of model robustness. DistLM was performed using normalised predictor variables selected in stepwise protocol and their influence evaluated in sequential tests with adjusted r^2 values. PRIMER 6/PERMANOVA+ (PRIMER-E Ltd) was used for all multivariate analyses, and one way ANOVA was calculated in Minitab 15. Data visualizations of OTU relative abundances using Microsoft Excel or PRIMER6/PERMANOVA and Adobe Illustrator are based upon unmodified data.

Network Analysis

A vector was created for each OTU to represent the OTU's abundance in each of the 37 samples as indicated by the formula:

$$x_i = [x_{i1}, x_{i2}, \dots, x_{i37}]\ (i = 1, \dots, 755)$$

To reduce sequencing effort bias, x_i values < 5 was set to zero (Zhang *et al.* 2013) and OTU vectors which contain less than 8 non-zero elements (20%) were removed to reduce false high correlations (Berry & Widder 2014). A second set of vectors was created based on environmental variables measured for each of the 37 samples. Pairwise Spearman correlations between all vectors were calculated and the associated p-value corrected for multiple comparisons with a Benjamini-Hochburg adjustment.

A community network was created based on significant correlations ($\rho>|0.7|$ and adjusted $p<0.05$) using package [iGraph] in R(Csardi & Nepusz 2006), incorporating both OTU abundances and measures of environmental variables. Community detection was based on random walk algorithm ("walktrap") in [iGraph] (Pons & Latapy 2005). Network parameters were compared with the Erdös-Renyi random model of a network of equal size. For both observed and random model communities, network parameters were calculated using the [iGraph] package in R (Csardi & Nepusz 2006).

To identify keystone taxa, the community network structure was used to identify OTUs which function as "bottlenecks" within the community, suggesting that they are central to community structuring and/or function. Bottlenecks are here defined as nodes with highest betweenness centrality, a count of the number times the bottleneck appears on the shortest paths between all other pairs of nodes (Peura *et al.* 2015) and therefore a measure of their connectivity within the co-occurrence network..

RESULTS

Semi-conductor sequencing of 16S rRNA genes from 37 cryoconite samples distributed over the Foxfonna ice cap (Figure 1) generated 4 609 547 total reads. Following processing, 755 bacterial OTUs were assigned by GreenGenes taxonomy to 13 phyla and 2 candidate phyla using a 97% similarity cut-off. It should be noted that results of preliminary T-RFLP community profiling of 16S rRNA genes cross-verified those of 16S sequencing in terms of spatial and environmental parameter prediction trends (data not shown) therefore T-RFLP results are not reported further.

Community composition and relative abundance of higher grade taxa

OTUs representing 87-91% of total relative abundance (RA) in the four sectors could be assigned to GreenGenes taxonomy (Figure 2; Supplementary Table 2). Across the cryoconite of Foxfonna ice cap the following phyla dominated the sequence dataset; *Proteobacteria* (28.3% RA), followed by *Actinobacteria* (21.8% RA), *Cyanobacteria* (18.4% RA), *Bacteroidetes* (7.0% RA), *Chloroflexi* (5.5% RA), *Gemmatimonadetes* (4.85% RA) and *Acidobacteria* (1.77% RA). Within individual sectors (Figure 2) *Proteobacteria* was the abundant phylum in sectors G1-G4 with RAs of 31.5%, 24.5%, 28.9%, 29.2% respectively. *Actinobacteria* on the other hand were the second most abundant in G1 (23.9% RA), G2 (22.9% RA) and G4 (24.7% RA). The phylum *Cyanobacteria* was second-most represented in the sequence data from sector G3 (21.7% RA) and third in sectors G1 (20.0 % RA), G2 (14.6% RA) and G4 (17.5% RA). Within the *Proteobacteria*, *Betaproteobacteria* dominated over other classes (16.2% RA) followed by *Alphaproteobacteria* (6.8% RA). No significant differences were observed in the diversity indices for species richness (ANOVA, F=0.4, p = 0.754) and evenness value (ANOVA, F=0.27, p=0.845) between sectors.

Evidence for a moderate pairwise distance-decay relationship in bacterial community structure

Potential pairwise distance-decay relationships in Bray-Curtis similarity of fourth-root transformed OTU relative abundance and geographic distance were tested for with 666 pairwise combinations of holes at distances between 77-1664 metres. The distance-decay plot of the overall community (Supplementary Figure 1) shows a weak relationship between geographical distance (m) and community dissimilarity which is confirmed by RELATE analysis, revealing a moderate spatial influence upon overall community structure (ρ=0.275, p=0.001). This is accounted for by significant Spearman correlations (Table 1) for the *Acidobacteria* (ρ=0.256, p=0.012), *Chloroflexi* (ρ=0.36, p=0.001), *Gemmatimonadetes* (ρ= 0.275, p = 0.025), *Proteobacteria* (ρ=0.188, p=0.045), and unassigned taxa (ρ=0.397, p=0.001).

Environmental influences on bacterial community structure

Canonical analysis of principal coordinates (Figure 3b) clearly differentiates between sectors of the ice cap, assigning 78.3% of samples to the correct sector upon leave-one out analysis. Moreover, PERMANOVA returns a highly significant sector effect (pseudo-F= 3.0622, p=0.001 with 999 permutations). Pairwise PERMANOVA (Supplementary Table 3) reveals each combination of sectors differ significantly (t=1.48-2.27, p=0.001-0.007) suggesting a clear effect of ice cap surface position on the bacterial community structure. When split by phylum, OTU relative abundances differed significantly for most phyla (Pseudo-F=2.43-5.74; p=0.001-0.007) between sectors with the exception of *Acidobacteria* and *Thermi.*

Therefore, to evaluate the relative importance of environmental factors in structuring the bacterial community, distance-based linear modelling (distLM; Figure 3a) was performed, resulting in a model which explained 29.2% of the total variation in the first two distance-based redundancy analysis axes. Stepwise selection of predicting variables identified significant contributions (p<0.01) by parameters related to geographic position (Northings, Eastings, elevation, slope and aspect), melting season duration (summer positive degree days and hours, positive hours, number of hours with incident radiation,) and biotic factors (chlorophyll *a* concentration and apparent cryoconite area) in marginal tests (Supplementary Table 4). Of these, sequential tests revealed positive degree days in summer as the most influential (contribution to adjusted r^2=0.12, pseudo-F=6.07, p=0.001) followed by slope (contribution to adjusted r^2=0.08, pseudo-F=4.93, p=0.001) Northings (contribution to adjusted r^2=0.001, pseudo-F=2.43, p=0.001), Apparent Cryoconite Area (contribution to adjusted r^2=0.03, pseudo-F=2.06, p=0. 01), and Eastings (contribution to adjusted r^2=0.04, pseudo-F=2.99, p=0.002). Wetness, FAA, incident radiation, positive degree hours and elevation did not contribute significantly (p>0.05) to the final model (adjusted r^2=0.33; r^2=0.52; Supplementary Table 5).

OTU occupancy analysis reveals the cryoconite bacterial community is dominated by a generalist core

To explore the distribution and dominance of specific bacterial taxa in cryoconite across the Foxfonna ice cap, the mean relative abundance of OTUs (clustered at 97%) across all samples was compared with the number of samples containing each OTU (i.e. occupancy; (Barberan *et* *al.* 2012)). A clear pattern emerges (Figure 4) in that the cryoconite bacterial community is strongly dominated by a small number of taxa. Of the 755 OTUs present in the dataset, only 16 OTUs are present at a mean RA per sample >1 %. The cross-sample cumulative RA of these 16 OTUs is strongly correlated with mean RA (Pearson r=0.99, p<0.0001) indicating minimal variation in their RA in sites across the ice cap. Strikingly, all 16 OTUs present at a mean RA per sample >1% are present in at least 36 of the 38 cryoconite samples analysed, and indeed in all 37 samples for 13 of those OTUs. Consequently, these 16 OTUs are collectively considered a group of core taxa which is both ubiquitous and abundant within the cryoconite bacterial community. BLAST-based closest environmental relatives (CER) and closest named relatives (CNR) of core taxa (Supplementary Table 6) reveals the core OTUs closely match uncultured sequences (CER %id 97-99%) mainly from cryospheric (13 OTUs) and soil (3 OTUs) habitats worldwide and more distantly related to cultivated taxa from soil (14 OTUs, CNR % id 88-98) plus Antarctic cyanobacteria (2 OTUs).

A long tail distribution of less abundant, variable occupancy, non-core taxa is also present (Figure 4). Across both core and tail populations, mean RA is positively correlated with occupancy (Spearman r=0.77, p<0.001). The tail population of the cryoconite bacterial community on Foxfonna comprises OTUs affiliated to at least 9 phyla, including the proteobacterial classes *Alpha-, Beta-, Delta* and *Gamma- proteobacteria.* The core OTUs include representatives of *Actinobacteria* (5 OTUs)*, Cyanobacteria* (2 OTUs)*, Proteobacteria* (one *Alphaproteobacteria* OTU, three *Betaproteobacteria* OTUs and one *Gammaproteobacteria* OTU) and single OTUs from each of *Bacteroidetes, Chloroflexi, Gemmatimonadetes* and an unassigned OTU. Of these OTUs, an OTU, denovo40205, assigned to the filamentous cyanobacterial genus *Leptolyngbya* is very prominent, being present in all 37 sites and at a mean RA (12.5%) four times greater than the next most dominant OTUs, an actinobacterial taxon affiliated to *Microbacteriaceae* and a *Betaproteobacteria* OTU, both present at 4.4-4.5% mean RA. All remaining core OTUs are present at 1.0-2.9% mean RA and include an OTU affiliated to the filamentous cyanobacterial genus *Phormidium* (1.14% mean RA, at 36 sites).

Core OTUs are stronger influences on tail and total OTU relative abundances than environmental conditions

The effect of core OTU composition and environmental parameters on tail and total OTU relative abundances was examined (Figure 5, Figure 6). Both core and tail OTU populations are significantly different in relative abundance across all quadrats of the Foxfonna ice cap (PERMANOVA; Pseudo-*F*=4.42, *p*=0.001; Pseudo-*F*=3.021, *p*=0.001 respectively; CAP shown in Figure 6 b-c). The Bray-Curtis distance matrices of core and tail OTU RA exhibit a much stronger correlation (RELATE; ρ=0.88, *p*=0.001) than to geographic distance (RELATE; ρ=0.29, *p*=0.01; ρ =0.27, *p*=0.001). Therefore the interactions between core and tail OTU populations with environmental parameters were examined with a view to understanding the relative importance of core taxa and environmental conditions in shaping the cryoconite bacterial community.

When applying distLM with a matrix of core OTU RAs as predictors of tail OTU RA patterns (Figure 6), all 16 core OTUs were very significant contributors (*p*=0.001-0.007) in marginal tests (Supplementary Table 7), with 10 of 16 core OTUs highly significant in the derived model according to sequential tests (Supplementary Table 8). For consistency, each core OTU is referred to by the most detailed taxonomic assignment made and the reference number of the OTU assigned during OTU selection. This model (adjusted r^2=0.57; r^2=0.76) is influenced most by an OTU assigned to *Sphingobacteriaceae* (hereafter referred to as

Sphingobacteriaceae-61341; contribution to adjusted r^2=0.15, pseudo-F=7.43, p=0.001) followed by *Microbacteriaceae*-32521 (contribution to adjusted r^2=0.11, pseudo-F=6.18, p=0.001), *Intrasporangiaceae*-46072 (contribution to adjusted r^2=0.10, pseudo-F=5.27, p=0.001) with *Chloroflexi*-37757, *Intrasporangiaceae*-27964, *Gemmatimonadales*-59904, *Phormidium*-45763, *Leptolyngbya*-40205, *Xanthomonadaceae*-51358 and *Betaproteobacteria*-10679 in decreasing order of influence, yet remaining statistically significant (Supplementary Table 8, p=0.001-0.025).

Considering the apparent strength of core OTU influence in shaping the tail population, the relative influence of the core and environmental parameters upon the total and tail OTU populations was tested (Figure 5, Figure 6). All 16 OTUs, and parameters relating to Cartesian position, chlorophyll content and apparent cryoconite area and melt season duration were significant predictors of total community structure (p<0.05) in marginal tests (Supplementary Table 9) while parameters relating to energy receipt and melt (e.g. incident radiation or wetness) were not, with the exception of hours of incident radiation. Sequential tests (Supplementary Table 10) revealed the derived model (adjusted r^2=0.60; r^2=0.84) was heavily influenced by seven core OTUs (cumulative r^2=0.59), principally *Sphingobacteriaceae*-61341 (contribution to adjusted r^2=0.17, pseudo-F=8.55, p=0.001) and *Microbacteriaceae*-32521 (contribution to adjusted r^2=0.13, pseudo-F=7.35, p=0.001) followed by OTUs assigned to *Intrasporangiaceae, Leptolyngbya, Chloroflexi* and *Phormidium* in decreasing order of influence. Subsequently, the three least influential (but still statistically significant) predictors in the sequential tests were environmental parameters relating to geographic position and hours of incident radiation (their cumulative adjusted r^2=0.04, pseudo-F=1.52-1.97, p=0.003-0.02). The strong trend for core OTU influence to predominate over the environmental parameters measured in shaping the bacterial community is clearly paralleled in distLM prediction of tail population OTUs (Sequential tests: SupplementaryTable 11, dbRDA plot: Figure 6, Marginal tests: Supplementary Table 12) with *Sphingobacteriaceae*-61341 (contribution to adjusted r^2=0.17, pseudo-F=8.35, p=0.001) and *Microbacteriaceae*-32521 (contribution to adjusted r^2=0.12, pseudo-F=7.05, p=0.001) again the strongest predicting variables of tail OTU structure. A total of 8 core OTUs plus three environmental parameters (Cartesian position, hours of incident radiation) are significant predictors of tail OTU structures.

OTU co-occurrence network analysis reveals modular sub-networks

Analysis of significant pairwise correlations between OTUs and environmental parameters resulted in a relatively small network with 145 nodes and 304 edges. The observed network was highly modular (observed = 0.77, Erdös-Renyi model = 0.41), with a considerably longer average path length than expected from a random model of the same size (observed = 4.93, Erdös-Renyi model = 3.58).

Environmental variables did not appear connected to most OTUs in the network, except for in the case of one small cluster of OTUs disconnected from the remaining network. This cluster was negatively correlated with several environmental variables related to energy inputs including positive degree day sum (PDD), hours with temperature above 0°C (PositiveHrs) and the positive degree day hours (PDhrs) (Figure 7).

The network contained several tightly clustered groups, disconnected or weakly connected with the remaining community (Figure 7). Though there is some clustering of phylogenetic groups, most groups are made up of OTUs from diverse taxa. Only one group is clearly determined by phylogeny consisting of a small cluster of OTUs in the phylum *Cyanobacteria*.

Bottleneck OTUs as identified by the highest betweenness centrality score were dominated by OTUs of the phylum *Actinobacteria* (top ten bottleneck OTUs: Table 2). All bottleneck OTUs were connected to the largest cluster within the network through positive correlations, with the exception of *Leptolyngbya*-40205. This OTU links a tight cluster of *Cyanobacteria* OTUs through a negative correlation to OTUs in the largest network cluster (Figure 7). Six of the ten top-scoring bottleneck OTUs are present within the core population (mean RA >1%).

DISCUSSION

The bacterial landscape of Foxfonna ice cap

Understanding the distributions of microbiota provides insights into the assembly, biogeography and function of microbial communities across multiple scales(Bell 2010; Bell *et al.* 2005). In the context of cryoconite ecosystems, understanding the spatial organization of community composition provides insights into the microbial colonization of an extreme environment, and the consequential interactions with melt responses of glacial ice surfaces.

Here we present the first bacterial biogeography of an ice cap. Semiconductor sequencing of bacterial 16S rRNA genes amplified from cryoconite ecosystems distributed across an Arctic ice cap reveals a cryoconite bacterial community dominated by a generalist core of (nearly-) ubiquitous OTUs which influence the total and tail (i.e. non-core) bacterial community structure. Chief among the core OTUs is a taxon assigned to the filamentous cyanobacterial genus *Leptolyngbya* by the GreenGenes taxonomy. Co-occurrence network analyses reveal a highly modular network which is constrained by bottleneck OTUs (Peura *et al.* 2015) exhibiting high betweenness centrality scores. The ten top scoring OTUs are also members of the core population. It is notable that the clearest phylogenetic signal within the network's modules is apparent in a module comprised solely of cyanobacterial OTUs

Linking diversity analyses with geographical and other environmental parameters extracted from a digital elevation model of the ice cap permits the elucidation of the physical factors governing the assembly and structure of cryoconite bacterial communities. Distance-based Linear Modelling reveals geographic position on the ice cap and melt season duration to be better predictors of bacterial community structure than parameters relating to energy receipt or surface hydrology. However, the structure of the core OTU population is a much better predictor of both total and tail community structure than the measured environmental parameters alone. The stronger influence of specific taxa rather than physical conditions on the Foxfonna cryoconite microbiota is reflected within network analyses. Only two modules within the network are linked to the physical parameters, but by negative correlations. The analyses presented are highly coherent with the notion that cryoconite bacterial communities develop as a consequence of autogenic ecosystem engineering (Cook *et al.* 2015b; Edwards *et al.* 2014b) in the form of granular aggregation (Hodson *et al.* 2010; Langford *et al.* 2010). The ubiquity and dominant abundance of OTU *Leptolyngbya*-40205 within the 16S sequencing data are particularly consistent with a role as an ecosystem engineer. (Musilova *et al.* 2015)

However, the prominence of heterotrophic bacteria within the core and bottleneck OTU populations is intriguing. In particular six OTUs assigned to the *Actinobacteria* accounting for six of the top scoring bottleneck OTUs and five of those are present within the core population. Of these, five are members of *Intrasporangiaceae.* While *Actinobacteria* have been detected in previous studies of cryoconite bacteria (Edwards *et al.* 2011; Edwards *et al.* 2014b) this is the first time their prominent role in structuring the cryoconite bacterial community has been invoked. Previous work has identified the predominance of *Alpha-* and *Beta- proteobacteria* within cryoconite microbiota (Edwards *et al.* 2014b; Stibal *et al.* 2015). While these are well-represented within the core population of Foxfonna cryoconite, they are conspicuously absent from the bottleneck OTUs. We therefore infer that while taxa from *Cyanobacteria* engineer the ecosystem and *Proteobacteria* contribute to heterotrophic processes, certain *Actinobacteria* play a contrasting role by mediating key processes or biotic interactions which affect overall community structure. Since keystone taxa are defined as taxa which show influence upon a community or ecosystem beyond that expected from their abundance(Power & Mills 1995) we consider these *Actinobacteria* OTUs as keystone taxa and that biotic factors may play a hitherto unrecognized role in the formation of cryoconite bacterial communities. Consequently, evaluating the relative roles of dispersal, environmental and biotic filters in shaping the cryoconite bacterial community is merited.

How does dispersal filtering shape this bacterial community?

Contemporary microbial ecology literature is replete with studies inspired by Baas-Becking's infamous statement (Baas-Becking 1934; De Wit & Bouvier 2006). A broad consensus may be that some taxa are indeed cosmopolitan, while others exhibit biogeographical trends (van der Gast 2015). For glaciers, the predominance of cosmopolitan taxa has been noted (Darcy *et al.* 2011; Franzetti *et al.* 2013) and previous work indicated distance-decay effects had negligible influence in shaping the cryoconite biota of neighbouring valley glaciers (Edwards *et al.* 2011). Since the Foxfonna ice cap is dome-shaped and not constrained by its surrounding topography to face a given aspect, unlike valley glaciers, we hypothesised that potential distance-decay effects would be revealed in this setting. Overall, there are statistically significant but moderate distance-decay effects which consistent for both core and tail populations, and are pronounced and significant for *Chloroflexi, Acidobacteria* and *Gemmatimonadetes* in clear contrast to other phyla. It may be that specific traits in the life history of these taxa condition their dispersal e.g.(Chu *et al.* 2011; DeBruyn *et al.* 2011).

Meanwhile, it is noteworthy that all core OTUs have closest environmental relatives exhibiting >97% identity along the V1-V3 region of the 16S rRNA gene present in samples from a global range of habitats which, with one exception, are from the cryosphere (Supplementary Table 6). Coupled with their ubiquity across the ice cap, most probably due to redistribution across the ice surface, this suggests an important trait of these core taxa is their broad distribution across the cryosphere, thus promoting their likelihood of colonization, resulting in a locally abundant and ubiquitous core population derived from a global pool of propagules.

How does environmental filtering influence this bacterial community?

The second clause of Baas-Becking's statement (Baas-Becking 1934) directs the reader's attention to the notion that prevailing environmental conditions influence microbial community composition. Countless studies certainly support the importance of abiotic factors in shaping microbial communities influenced by deterministic processes (e.g. (Wood *et al.* 2008)). The influence of surface hydrology and distance from the ice margin have been inferred for valley glacier and ice sheet microbiota respectively (Edwards *et al.* 2011; Stibal *et al.* 2015). Here, distLM consistently invoked physical parameters relating to geographic position and melting season duration (either as positive degree days, Supplementary Table 5; or hours of incident radiation, Supplementary Table 11) as the strongest significant predictors of community structures.

A common feature of all models was that factors relating to surface hydrology, either as wetness of the ice surface or the extent of the FAA, failed to predict community structure. Within the context of the Foxfonna ice cap, which resides at higher elevation and latitude, with low mass balance gradients that exhibit strong inter-annual variability, this is plausible. These conditions mean that community development may be curtailed to relatively brief seasons of predominantly bare ice with a limited evolution of surface hydrological networks and porous weathering crust ice at the surface, in contrast to cryoconite situated on strongly ablating ice with longer growing seasons (Cook *et al.* 2015c; Irvine-Fynn & Edwards 2013). While temporal analyses of cryoconite microbiota at the margin of the Greenland ice sheet imply overall stability in community structure within melting seasons (Musilova *et al.* 2015) we infer that the overall duration of melting season is an influential environmental parameter. Further studies should directly examine the temporal evolution of cryoconite community structures, particularly in conditions beyond those typical of the southwestern margin of Greenland's ice sheet, and in so doing challenge the potential over-simplification of current global models of cryoconite carbon cycling, which assume uniform rates of productivity across a melting season of fixed duration (for example, 70 days: Anesio, *et al.,* (2009)).

How does biotic filtering in the form of taxon interactions influence the bacterial community?

Recognition that biotic filtering (i.e. taxon-taxon interactions such as competition, cooperation and indeed ecosystem engineering) is an influential driver in the assembly of environmental microbial communities is much more recent e.g. Goberna *et al.,* (2014). In the context of glacial ecosystems, discourse regarding biotic filtering has been limited to identifying algal taxa as primary colonizers of glacial surfaces e.g. Lutz *et al.* (2015) or the role of filamentous cyanobacteria as putative ecosystem engineers or keystone species (Edwards *et al.* 2014b). Here, we deduce that taxon interactions drive the assembly of cryoconite communities colonizing the Foxfonna ice cap. The composition of the core bacterial taxa is a strong predictor of the total and tail bacterial populations, with the distributions of specific taxa proving better predictors than any physical parameters. Moreover, the highly modular co-occurrence network is structured by nodes acting as bottleneck OTUs (Table 2).

Congruent with prior work (Hodson *et al.* 2010; Langford *et al.* 2010), we find filamentous cyanobacteria, specifically the OTU *Leptolyngbya*-40205 are important in the cryoconite bacterial community, but while we concur they represent autogenic ecosystem engineers

(Edwards *et al.* 2014b; Langford *et al.* 2010; West 1990) they are less prominent as keystone taxa. In contrast, selected *Actinobacteria* OTUs are prominent, highly-centralized bottleneck OTUs within the highly modular co-occurrence network observed (Figure 6). We infer these represent keystone taxa in that their influence exceeds their relative abundance within the community profiled. Their positive co-occurrence with other taxa mitigates against their role in competitive exclusion. Since their closest named relatives (Supplementary Table 6) comprise taxa associated with soil humus we speculate these taxa may play roles in the humification of dark organic matter associated with cryoconite (Takeuchi *et al.* 2001).

Others have interpreted phylogenetic clustering as evidence for biotic filtering (Goberna *et al.* 2014). The co-occurrence network derived here is modular in its nature, with taxonomically diverse modules, a characteristic in common with taxon co-occurrence networks established for other polar habitats, and interpreted as a sign of metabolic plasticity (Vick-Majors *et al.* 2014). Thus, the predominance of phylogenetically diverse modules may permit the functional stability of the community in the face of its fluctuating environment. Most of these modules exhibit phylum-level diversity with the exception of an exclusively cyanobacterial module which is negatively correlated with the largest module, which houses all remaining bottleneck OTUs. The disposition of the cyanobacterial module suggests that the autogenic ecosystem engineers exert a limited influence upon community structure, unlike heterotrophic bottleneck OTUs. Therefore, we contend that filamentous cyanobacteria, having engineered the cryoconite ecosystem by the aggregation of aeolian organic matter and inorganic debris (Hodson *et al.* 2010; Langford *et al.* 2010) are disconnected from the heterotrophic bacterial community, which comprises closely interacting taxa. As such, the assembly of the cryoconite bacterial community is biotically filtered with a primary succession from phototrophic taxa associated with granule formation towards a highly interactive consortium of heterotrophic bacteria which may act to humify the accumulated organic matter.

Technical considerations and limitations of the present study

This study focuses upon the intensive coverage of one ice cap in the High Arctic at a single time-point and targets the bacterial community only. We note the presence of eukaryote and viral communities in cryoconite(Säwström *et al.* 2002), beyond the scope of this study, as well as reliable reports of Archaea associated with cryoconite, albeit from alpine and Antarctic cryoconite(Cameron *et al.* 2012; Hamilton *et al.* 2013). The amplicon sequencing dataset generated within this study did not reveal the presence of Archaea, and PCR assays targeting Archaea did not generate specific amplicons (data not shown.) In line with other work suggesting that Archaea are not detected in Arctic cryoconite (Cameron *et al.* 2012; Edwards *et al.* 2011) we focused upon the bacterial community. Furthermore, analyses of multiple time points and localities are likely to yield further insights to the structure and function of glacial ecosystems (Edwards & Cook 2015). However, recent studies implying the temporal stability of bacterial communities in cryoconite ecosystems (Musilova *et al.* 2015), coupled with the cosmopolitan distribution of core taxa (Supplementary Table 6) documented in a variety of cryospheric habitats imply the broader utility of insights from the Foxfonna ice cap. The importance of melt season duration as a physical parameter predicting the bacterial community structure is noted, and thus examination of cryoconite ecosystems in discrete stages of melt season conditions is recommended, since this study sampled during the late melt season.

Bulk DNA extraction coupled with amplicon semiconductor sequencing of the 16S rRNA gene has been employed, in line with many other contemporary studies in microbial ecology

(Prosser 2012). Necessarily these studies all entail systematic biases in extraction, amplification and sequencing (Lee *et al.* 2012). An important caveat here is that bulk DNA extracts will include templates from active and inactive taxa (Blazewicz *et al.* 2013; Klein 2015) and thus the detection of temporal variation in activity levels is precluded (Stibal *et al.* 2015). Finally, processed reads were aligned to the GreenGenes taxonomy as described. It should be noted that the highly dominant OTU, *Leptolyngbya*-40205, assigned to the genus *Leptolyngbya* within the GreenGenes taxonomy possesses a closest named relative within an Antarctic strain *Phormidesmis priestleyi* (95% id AY493581) which is also the closest relative of Sanger-sequenced clone library Oscillatorean cyanobacterial OTUs from cryoconite elsewhere on Svalbard (Edwards *et al.* 2011) and dominates the active bacterial community of cryoconite on the south-western margin of the Greenland Ice Sheet (Cook *et al.* 2016). As the phylogenetic placement of cyanobacteria from the cold biosphere improves (Chrismas *et al.* 2015), so will the taxonomic affiliation of this cryoconite ecosystem engineer, which currently resides within the *Phormidesmis*-like clade of cold adapted cyanobacteria.

Summary

We conclude that the assembly of the bacterial community of microbial-mineral aggregates colonizing the High Arctic ice cap of Foxfonna is driven principally by biotic filtering. A dominant generalist core of taxa emerges which includes filamentous cyanobacterial ecosystem engineers and a discrete group of keystone taxa principally within the *Actinobacteria,* likely humifying accumulated organic matter to darken the cryoconite. While there is evidence for a moderate distance-decay effect in community similarity, it is notable that the core taxa possess close environmental relatives from the global cryosphere, linking microbial colonization processes interacting with glacier change at local scales with dispersal within the cosmopolitan cold biosphere (Jungblut *et al.* 2009).

ACKNOWLEDGEMENTS

We gratefully acknowledge NERC NE/K000942/1 and AU University Research Fund to AE; Great Britain Sasakawa Foundation to AE, NT, TI-F; NERC NE/G006253/1 to AJH; Welsh Livery Guild scholarship to JSB; South African National Research Foundation Fellowship to JKG. All authors thank the staff and students at UNIS for assistance with sample collection.

DATA ACCESSIBILITY

Sequence data are available at EBI-SRA (SRP067436 : PRJNA306097).

AUTHOR CONTRIBUTIONS

Conceived study: AJH, JKG, AE; conducted fieldwork: AE, TIF, JSB, NT, AJH; conducted labwork: AE, JKG, PJW, APD; conducted data analyses: JKG ERS TIF LAJM AE; wrote manuscript: JKG, ERS, TIF, AE. All authors contributed to and approved manuscript submission.

TABLES AND FIGURES

TABLE 1: Spearman correlation between matrices of physical and Bray-Curtis distance by phylum provided via RELATE analysis; significant correlations highlighted.

TABLE 2: Network bottlenecks identified as the OTUs with highest betweenness centrality metrics. Node ID matches that used in figure 7.

FIGURE 1: Map of study location, the Foxfonna ice cap on Svalbard with (A) aerial overview and (B) extracted digital elevation model, indicating sample points according to sector within the figure key.

FIGURE 2: Phylum-level composition of 16S rRNA genes profiled by amplicon semi-conductor sequencing and assigned to higher-grade taxa according to the GreenGenes taxonomy (A) Sector G1; (B) Sector G2; (C) Sector G3; (D) Sector G4. The category "Others" concatenates phyla present at a cumulative relative abundance <1% across the dataset (Armatimonadetes, GN02, OD1, Thermi).

FIGURE 3: Ordination based analyses of Foxfonna ice cap bacterial communities (A) distance-based redundancy analysis (dbRDA) ordination plot of distance-based linear models of physical parameter predictors of bacterial community structure; (B) Canonical Analysis of Principal Co-ordinates (CAP) of bacterial community structure according to a sector-based model.

FIGURE 4: Occupancy plotting reveals that the Foxfonna ice cap cryoconite bacterial communities (A) are dominated by a core of generalist taxa highlighted by box (exploded view of core in inset B, annotated with OTU references). Bubble size is proportional to $\log_{10}$ of total RA and bubbles are shaded by taxonomic affiliation. Occupancy is defined by the presence of an OTU within a site.

FIGURE 5: Distance-based redundancy analysis (dbRDA) ordination plot of distance-based linear models (A) core OTU and environmental parameters on total community and (B) core OTU and environmental parameters on tail community structure.

FIGURE 6: Distance-based redundancy analysis (dbRDA) ordination plot of distance-based linear models (A) of core predictors of tail community structure and Canonical Analysis of

Principal Co-ordinates (CAP) of core and tail (panels B and C respectively) community structures according to sector.

FIGURE 7: Community network based on significant pairwise Spearman correlations between OTUs (green – positive correlation, orange – negative correlation). Size of node is relative to average OTU abundance, while colour indicates OTU's phylum. Environmental variables have been included as nodes in the network and are indicated as black squares.

Table 1: Spearman correlation between matrices of physical and Bray-Curtis distance by phylum provided via RELATE analysis; significant correlations highlighted.

Phylum	**Rho**	***p* value**
Acidobacteria	0.256	**0.012**
Actinobacteria	0.123	0.114
Armatimonadetes	-0.019	0.549
Bacteroidetes	0.113	0.141
Chloroflexi	0.36	**0.001**
Cyanobacteria	0.154	0.065
Gemmatimonadetes	0.219	**0.025**
TM7	0.146	0.063
Proteobacteria	0.188	**0.045**
Thermi	0.094	0.174
Unassigned	0.397	**0.001**
WPS-2	0.079	0.233
OD1	0.086	0.203
GN02	-0.111	0.887

Table 2 Network bottlenecks identified as the OTUs with highest betweenness centrality metrics. Node ID matches that used in figure 7.

Node ID	OTU	Phylum	Class	Order	Family	Genus	Centrality	Mean RA>1
D220	Denovo61555	*Actinobacteria*	*Acidimicrobiia*	*Acidimicrobiales*	C111		1318	
D106	Denovo37757	Chloroflexi	C0119				1261	+
D187	Denovo53638	*Actinobacteria*	*Actinobacteria*	*Actinomycetales*	*Intrasporangiaceae*		1102	+
D17	Denovo1447	*Actinobacteria*	*Actinobacteria*	*Actinomycetales*	*Intrasporangiaceae*		973	+
D175	Denovo51679	*Gemmatimonadetes*	*Gemmatimonadetes*	*Gemmatimonadales*	Ellin5301		915	
D160	Denovo48894	*Actinobacteria*	*Acidimicrobiia*	*Acidimicrobiales*	EB1017		660	+
D121	Denovo40205	*Cyanobacteria*	*Synechococcophycideae*	*Pseudanabaenales*	*Pseudanabaenaceae*	*Leptolyngbya*	619	+
D73	Denovo27964	*Actinobacteria*	*Actinobacteria*	*Actinomycetales*	*Intrasporangiaceae*		617	+
D185	Denovo53430						552	
D125	Denovo41255	*Actinobacteria*	*Actinobacteria*	*Actinomycetales*	*Intrasporangiaceae*		536	

REFERENCES

Anesio AM, Hodson AJ, Fritz A, Psenner R, Sattler B (2009) High microbial activity on glaciers: importance to the global carbon cycle. *Global Change Biology* **15**, 955-960.

Baas-Becking LGM (1934) *Geobiologie; of inleiding tot de milieukunde* WP Van Stockum & Zoon NV.

Barberan A, Bates ST, Casamayor EO, Fierer N (2012) Using network analysis to explore co-occurrence patterns in soil microbial communities. *Isme j* **6**, 343-351.

Bell T (2010) Experimental tests of the bacterial distance-decay relationship. *ISME Journal* **4**, 1357-1365.

Bell T, Ager D, Song JI*, et al.* (2005) Larger islands house more bacterial taxa. *Science* **308**, 1884-1884.

Benn D, Evans DJ (2014) *Glaciers and glaciation* Routledge.

Berry D, Widder S (2014) Deciphering microbial interactions and detecting keystone species with co-occurrence networks. *Frontiers in Microbiology* **5**.219

Blazewicz SJ, Barnard RL, Daly RA, Firestone MK (2013) Evaluating rRNA as an indicator of microbial activity in environmental communities: limitations and uses. *The ISME Journal* **7**, 2061-2068.

Bøggild C (1997) Different melt regimes indicated by surface albedo measurements at the Greenland ice sheet margin–application of TM image. *EARSeL. Advances in remote sensing* **5**, 82-88.

Cameron KA, Hodson AJ, Osborn AM (2012) Structure and diversity of bacterial, eukaryotic and archaeal communities in glacial cryoconite holes from the Arctic and the Antarctic. *FEMS microbiology ecology* **82**, 254-267.

Caporaso JG, Kuczynski J, Stombaugh J*, et al.* (2010) QIIME allows analysis of high-throughput community sequencing data. *Nature Methods* **7**, 335-336.

Chrismas NAM, Anesio A, Sanchez-Baracaldo P (2015) Multiple adaptations to polar and alpine environments within cyanobacteria: a phylogenomic and Bayesian approach. *Frontiers in Microbiology* **6**, 1070.

Chu H, Fierer N, Lauber CL*, et al.* (2011) Soil bacterial diversity in the Arctic is not fundamentally different from that found in other biomes. *Environmental Microbiology* **12**, 2998-3006.

Cook J, Edwards A, Bulling M*, et al.* (2016) Metabolome-mediated biocryomorphic evolution promotes carbon fixation in Greenlandic cryoconite holes. *Environmental Microbiology* Accepted article: DOI: 10.1111/1462-2920.13349.

Cook J, Edwards A, Hubbard A (2015a) Biocryomorphology: integrating microbial processes with ice surface hydrology, topography and roughness. *Frontiers in Earth Science* **3**.

Cook JM, Edwards A, Takeuchi N, Irvine-Fynn TDL (2015b) Cryoconite: the dark biological secret of the cryosphere. *Progress in Physical Geography* **46,** 66-111.

Cook JM, Hodson AJ, Irvine-Fynn TDL (2015c) Supraglacial weathering crust dynamics inferred from cryoconite hole hydrology. *Hydrological Processes*, **30,** 433–446.

Csardi G, Nepusz T (2006) The igraph software package for complex network research. *InterJournal, Complex Systems* **1695**, 1-9.

Darcy JL, Lynch RC, King AJ, Robeson MS, Schmidt SK (2011) Global Distribution of *Polaromonas* Phylotypes - Evidence for a Highly Successful Dispersal Capacity. *Plos One* **6**, e23742.

De Wit R, Bouvier T (2006) ‘Everything is everywhere, but, the environment selects’; what did Baas Becking and Beijerinck really say? *Environmental Microbiology* **8**, 755-758.

DeBruyn JM, Nixon LT, Fawaz MN, Johnson AM, Radosevich M (2011) Global biogeography and quantitative seasonal dynamics of *Gemmatimonadetes* in soil. *Applied and Environmental Microbiology* **77**, 6295-6300.

DeSantis TZ, Hugenholtz P, Larsen N*, et al.* (2006) Greengenes, a chimera-checked 16S rRNA gene database and workbench compatible with ARB. *Applied and Environmental Microbiology* **72**, 5069-5072.

Edgar RC (2010) Search and clustering orders of magnitude faster than BLAST. *Bioinformatics* **26**, 2460-2461.

Edwards A, Anesio AM, Rassner SM*, et al.* (2011) Possible interactions between bacterial diversity, microbial activity and supraglacial hydrology of cryoconite holes in Svalbard. *The ISME Journal* **5**, 150-160.

Edwards A, Cook S (2015) Microbial dynamics in glacier forefield soils show succession is not just skin deep. *Molecular Ecology* **24**, 963-966.

Edwards A, Irvine-Fynn T, Mitchell AC, Rassner SME (2014a) A germ theory for glacial systems? *Wiley Interdisciplinary Reviews: Water*. **1,** 331–340

Edwards A, Mur LAJ, Girdwood S*, et al.* (2014b) Coupled cryoconite ecosystem structure-function relationships are revealed by comparing bacterial communities in Alpine and Arctic glaciers *FEMS Microbiology Ecology* **89**, 222-237.

Edwards A, Pachebat JA, Swain M*, et al.* (2013a) A metagenomic snapshot of taxonomic and functional diversity in an alpine glacier cryoconite ecosystem. *Environmental Research Letters* **8**, 035003.

Edwards A, Rassner SM, Anesio AM*, et al.* (2013b) Contrasts between the cryoconite and ice-marginal bacterial communities of Svalbard glaciers. *Polar Research* **32**, 19468.

Franzetti A, Tatangelo V, Gandolfi I*, et al.* (2013) Bacterial community structure on two alpine debris-covered glaciers and biogeography of Polaromonas phylotypes. *The ISME Journal* **7**, 1483–1492

Fuhrman JA (2009) Microbial community structure and its functional implications. *Nature* **459**, 193-199.

Goberna M, García C, Verdú M (2014) A role for biotic filtering in driving phylogenetic clustering in soil bacterial communities. *Global Ecology and Biogeography* **23**, 1346-1355.

Griffiths RI, Whiteley AS, O'Donnell AG, Bailey MJ (2000) Rapid Method for Coextraction of DNA and RNA from Natural Environments for Analysis of Ribosomal DNA- and rRNA-Based Microbial Community Composition. *Applied and Environmental Microbiology* **66**, 5488-5491.

Hamilton TL, Peters JW, Skidmore ML, Boyd ES (2013) Molecular evidence for an active endogenous microbiome beneath glacial ice. *The ISME Journal, 7***,** 1402-12.

Hill R, Saetnan ER, Scullion J*, et al.* (2015) Temporal and spatial influences incur reconfiguration of Arctic heathland soil bacterial community structure. *Environmental Microbiology doi: 10.1111/1462-2920.13017.*

Hock R (2005) Glacier melt: a review of processes and their modelling. *Progress in Physical Geography* **29**, 362-391.

Hodson A, Anesio AM, Ng F*, et al.* (2007) A glacier respires: quantifying the distribution and respiration CO_2 flux of cryoconite across an entire Arctic supraglacial ecosystem. *Journal of Geophysical Research* **112**, 9pp.

Hodson A, Anesio AM, Tranter M, *et al.* (2008) Glacial ecosystems. *Ecological Monographs* **78**, 41-67.

Hodson A, Cameron K, Bøggild C, *et al.* (2010) The structure, biogeochemistry and formation of cryoconite aggregates upon an Arctic valley glacier; Longyearbreen, Svalbard. *Journal of Glaciology* **56**, 349-362.

Hood E, Battin TJ, Fellman J, O'Neel S, Spencer RGM (2015) Storage and release of organic carbon from glaciers and ice sheets. *Nature Geoscience* **8**, 91-96.

Irvine-Fynn TDL, Bridge JW, Hodson AJ (2010) Rapid quantification of cryoconite: granule geometry and in situ supraglacial extents, using examples from Svalbard and Greenland. *Journal of Glaciology* **56**, 297-308.

Irvine-Fynn TDL, Edwards A (2013) A frozen asset: The potential of flow cytometry in constraining the glacial biome. *Cytometry part A* **85**, 3-7.

Irvine-Fynn TDL, Hodson AJ, Moorman BJ, Vatne G, Hubbard AL (2011) Polythermal glacier hydrology: A review. *Reviews in Geophysics.* **49**, RG4002.

Irvine-Fynn TD, Hanna E, Barrand N, *et al.* (2014) Examination of a physically based, high-resolution, distributed Arctic temperature-index melt model, on Midtre Lovénbreen, Svalbard. *Hydrological Processes* **28**, 134-149.

Jenson SK, Domingue JO (1988) Extracting topographic structure from digital elevation data for geographic information system analysis. *Photogrammetric engineering and remote sensing* **54**, 1593-1600.

Jungblut AD, Lovejoy C, Vincent WF (2009) Global distribution of cyanobacterial ecotypes in the cold biosphere. *The ISME Journal* **4**, 191-202.

Klein DA (2015) Partial Formalization: An Approach for Critical Analysis of Definitions and Methods Used in Bulk Extraction-Based Molecular Microbial Ecology. *Open Journal of Ecology* **5**, 400.

Langford H, Hodson A, Banwart S, Bøggild C (2010) The microstructure and biogeochemistry of Arctic cryoconite granules. *Annals of Glaciology* **51**, 87-94.

Langford HJ, Irvine-Fynn TDL, Edwards A, Banwart SA, Hodson AJ (2014) A spatial investigation of the environmental controls over cryoconite aggregation on Longyearbreen glacier, Svalbard. *Biogeosciences* **11**, 5365-5380.

Lee CK, Herbold CW, Polson SW*, et al.* (2012) Groundtruthing next-gen sequencing for microbial ecology–biases and errors in community structure estimates from PCR amplicon pyrosequencing.

Lutz S, Anesio AM, Edwards A, Benning LG (2015) Microbial diversity on Icelandic glaciers and ice caps. *Frontiers in Microbiology* **6**. 307.

Moore ID, Grayson R, Ladson A (1991) Digital terrain modelling: a review of hydrological, geomorphological, and biological applications. *Hydrological Processes* **5**, 3-30.

Musilova M, Tranter M, Bennett SA, Wadham JL, Anesio A (2015) Stable microbial community composition on the Greenland Ice Sheet. *Frontiers in Microbiology* **6**. 193

Pedrós-Alió C (2006) Marine microbial diversity: can it be determined? *Trends in microbiology* **14**, 257-263.

Peura S, Bertilsson S, Jones RI, Eiler A (2015) Resistant Microbial Cooccurrence Patterns Inferred by Network Topology. *Applied and Environmental Microbiology* **81**, 2090-2097.

Pons P, Latapy M (2005) Computing communities in large networks using random walks. In: *Computer and Information Sciences-ISCIS 2005*, pp. 284-293. Springer.

Power ME, Mills LS (1995) The keystone cops meet in Hilo. *Trends in Ecology & Evolution* **10**, 182-184.

Prosser JI (2012) Ecosystem processes and interactions in a morass of diversity. *FEMS Microbiology Ecology* **81**, 507-519.

Rime T, Hartmann M, Brunner I*, et al.* (2015) Vertical distribution of the soil microbiota along a successional gradient in a glacier forefield. *Molecular Ecology* **24**, 1091-108.

Rutter N, Hodson A, Irvine-Fynn T, Solas MK (2011) Hydrology and hydrochemistry of a deglaciating high-Arctic catchment, Svalbard. *Journal of Hydrology* **410**, 39-50.

Säwström C, Mumford P, Marshall W, Hodson A, Laybourn-Parry J (2002) The microbial communities and primary productivity of cryoconite holes in an Arctic glacier (Svalbard 79°N). *Polar Biology* **25**, 591-596.

Schloss PD, Westcott SL, Ryabin T*, et al.* (2009) Introducing mothur: open-source, platform-independent, community-supported software for describing and comparing microbial communities. *Applied and Environmental Microbiology* **75**, 7537-7541.

Segawa T, Ishii S, Ohte N*, et al.* (2014) The nitrogen cycle in cryoconites: naturally occurring nitrification-denitrification granules on a glacier. *Environmental Microbiology* **16**, 3250-3262.

Steele JA, Countway PD, Xia L*, et al.* (2011) Marine bacterial, archaeal and protistan association networks reveal ecological linkages. *The ISME Journal* **5**, 1414-1425.

Stibal M, Schostag M, Cameron KA*, et al.* (2015) Different bulk and active bacterial communities in cryoconite from the margin and interior of the Greenland ice sheet. *Environmental Microbiology Reports* **7**, 293-300.

Takeuchi N (2002) Optical characteristics of cryoconite (surface dust) on glaciers: the relationship between light absorency and the property of organic matter contained in the cryoconite. *Annals of Glaciology* **34**, 409-414.

Takeuchi N, Kohshima S, Seko K (2001) Structure, formation, and darkening process of albedo-reducing material (cryoconite) on a Himalayan glacier: a granular algal mat growing on the glacier. *Arctic Antarctic and Alpine Research* **33**, 115-122.

Tarboton DG (1997) A new method for the determination of flow directions and upslope areas in grid digital elevation models. *Water resources research* **33**, 309-319.

van der Gast CJ (2015) Microbial biogeography: the end of the ubiquitous dispersal hypothesis? *Environmental Microbiology* **17**, 544-546.

Vick-Majors TJ, Priscu JC, Amaral-Zettler LA (2014) Modular community structure suggests metabolic plasticity during the transition to polar night in ice-covered Antarctic lakes. *The ISME Journal* **8**, 778-789.

Wadham J, Kohler J, Hubbard A, Nuttall AM, Rippin D (2006) Superimposed ice regime of a high Arctic glacier inferred using ground-penetrating radar, flow modeling, and ice cores. *Journal of Geophysical Research: Earth Surface (2003–2012)* **111**.

Wang Q, Garrity GM, Tiedje JM, Cole JR (2007) Naive Bayesian classifier for rapid assignment of rRNA sequences into the new bacterial taxonomy. *Applied and Environmental Microbiology* **73**, 5261-5267.

West NE (1990) *Structure and Function of Microphytic Soil Crusts in Wildland Ecosystems of Arid to Semi-arid Regions* Academic Press.

Wise S (2000) Assessing the quality for hydrological applications of digital elevation models derived from contours. *Hydrological Processes* **14**, 1909-1929.

Wood SA, Rueckert A, Cowan DA, Cary SC (2008) Sources of edaphic cyanobacterial diversity in the Dry Valleys of Eastern Antarctica. *The ISME Journal* **2**, 308-320.

Zhang S-W, Wei Z-G, Zhou C, Zhang Y-C, Zhang T-H (2013) Exploring the interaction patterns in seasonal marine microbial communities with network analysis, 7th International Conference on Systems Biology (ISB) 63-68. DOI: 10.1109/ISB.2013.6623795

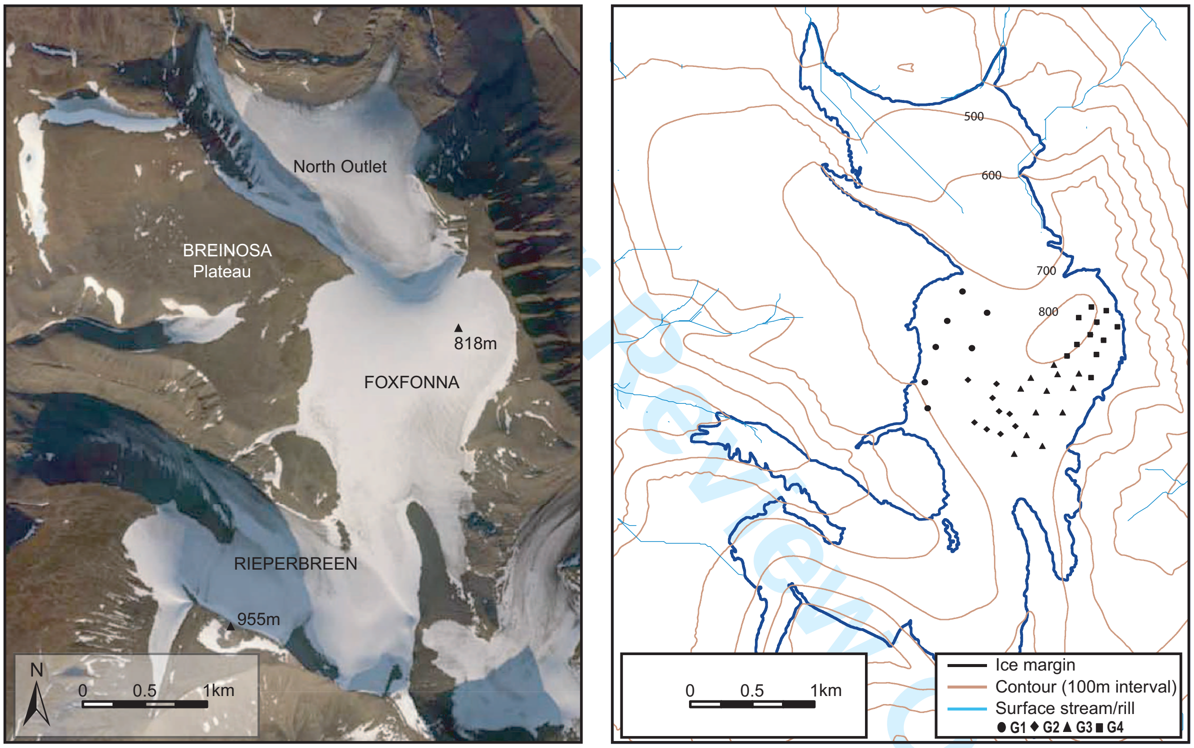
North Outlet
BREINOSA
Plateau
818m
FOXFONNA
RIEPERBREEN
955m
N
0 0.5 1km
500
600
700
800
0 0.5 1km
Ice margin
Contour (100m interval)
Surface stream/rill
● G1 ◆ G2 ▲ G3 ■ G4

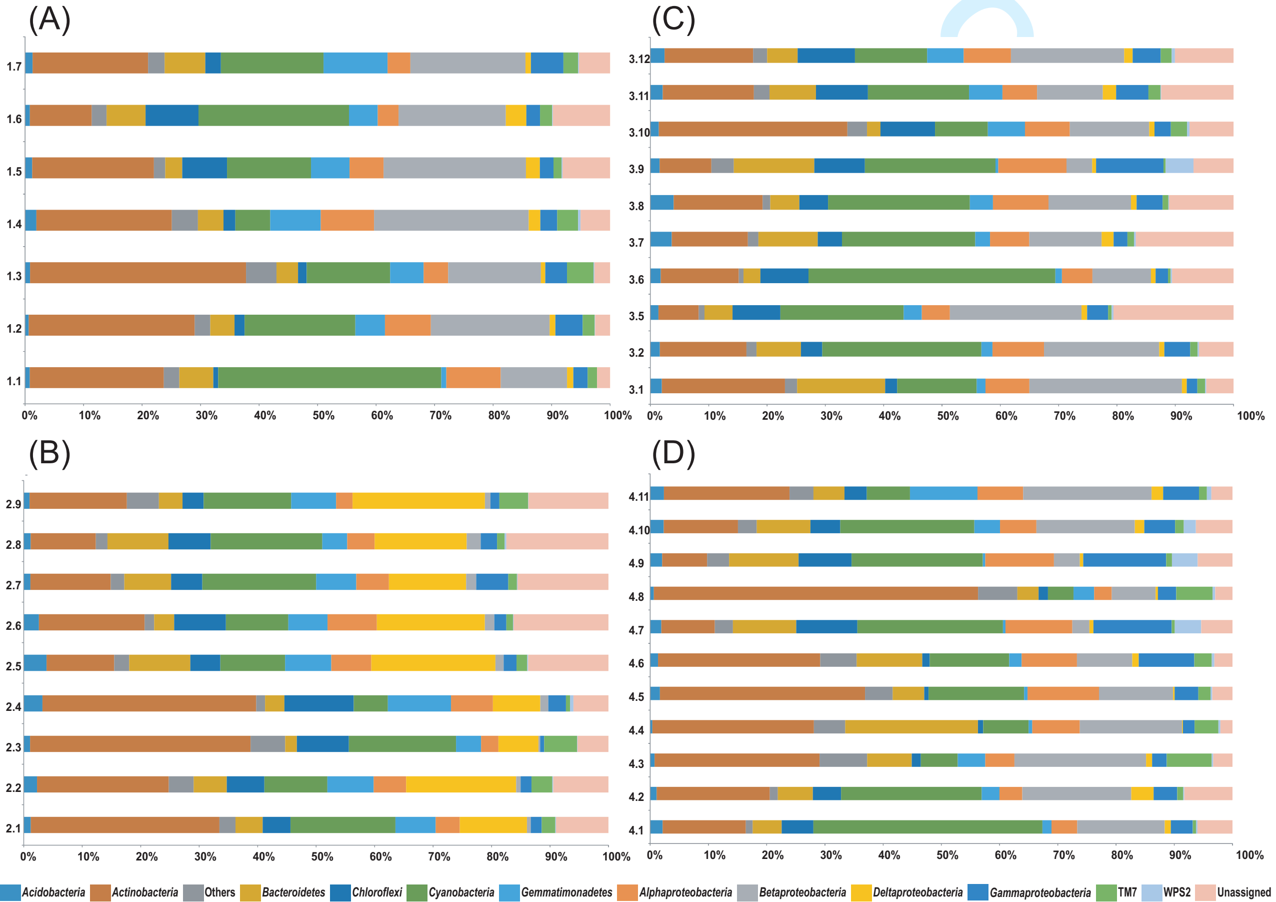
(A)
1.7
1.6
1.5
1.4
1.3
1.2
1.1
(C)
3.12
3.11
3.10
3.9
3.8
3.7
3.6
3.5
3.2
3.1
(B)
2.9
2.8
2.7
2.6
2.5
2.4
2.3
2.2
2.1
(D)
4.11
4.10
4.9
4.8
4.7
4.6
4.5
4.4
4.3
4.2
4.1
0%
10%
20%
30%
40%
50%
60%
70%
80%
90%
100%
Acidobacteria
Actinobacteria
Others
Bacteroidetes
Chloroflexi
Cyanobacteria
Gemmatimonadetes
Alphaproteobacteria
Betaproteobacteria
Deltaproteobacteria
Gammaproteobacteria
TM7
WPS2
Unassigned

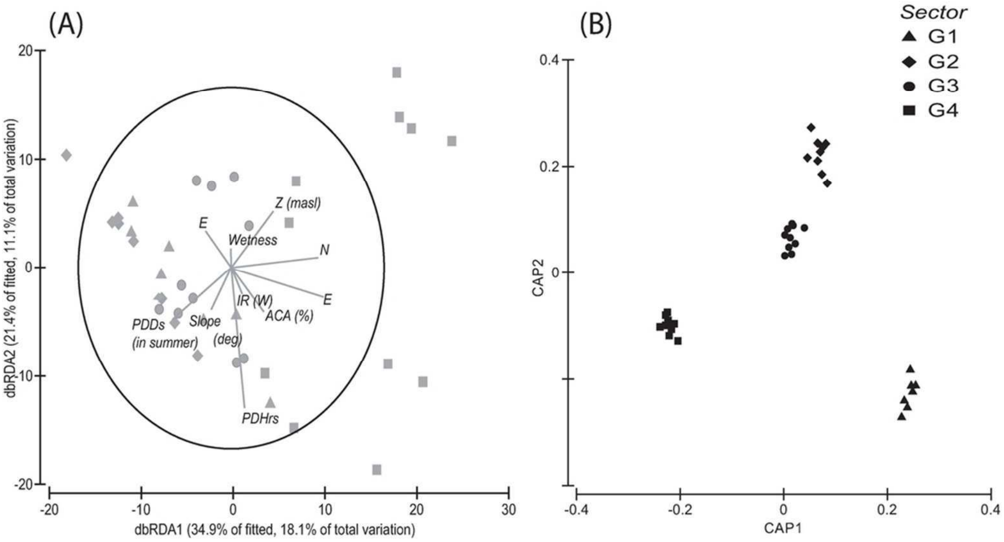

Ordination based analyses of Foxfonna ice cap bacterial communities (A) distance-based redundancy analysis (dbRDA) ordination plot of distance-based linear models of physical parameter predictors of bacterial community structure; (B) Canonical Analysis of Principal Co-ordinates (CAP) of bacterial community structure according to a sector-based model.
90x48mm (300 x 300 DPI)

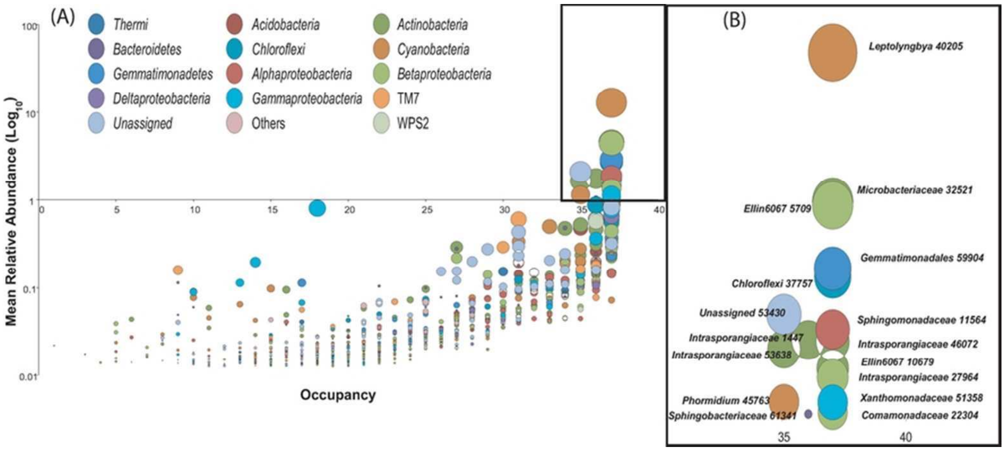

Occupancy plotting reveals that the Foxfonna ice cap cryoconite bacterial communities (A) are dominated by a core of generalist taxa highlighted by box (exploded view of core in inset B, annotated with OTU references). Bubble size is proportional to log10 of total RA and bubbles are shaded by taxonomic affiliation. Occupancy is defined by the presence of an OTU within a site.
74x33mm (300 x 300 DPI)

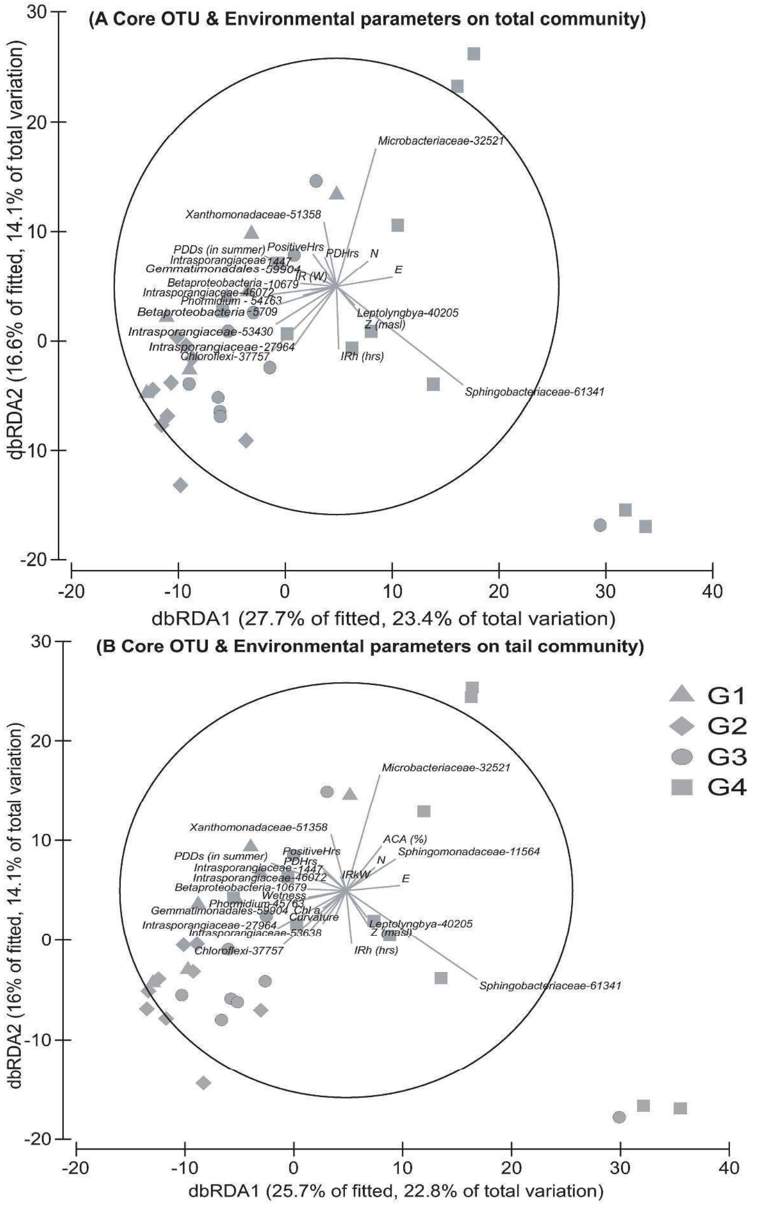

Distance-based redundancy analysis (dbRDA) ordination plot of distance-based linear models (A) core OTU and environmental parameters on total community and (B) core OTU and environmental parameters on tail community structure.

246x396mm (300 x 300 DPI)

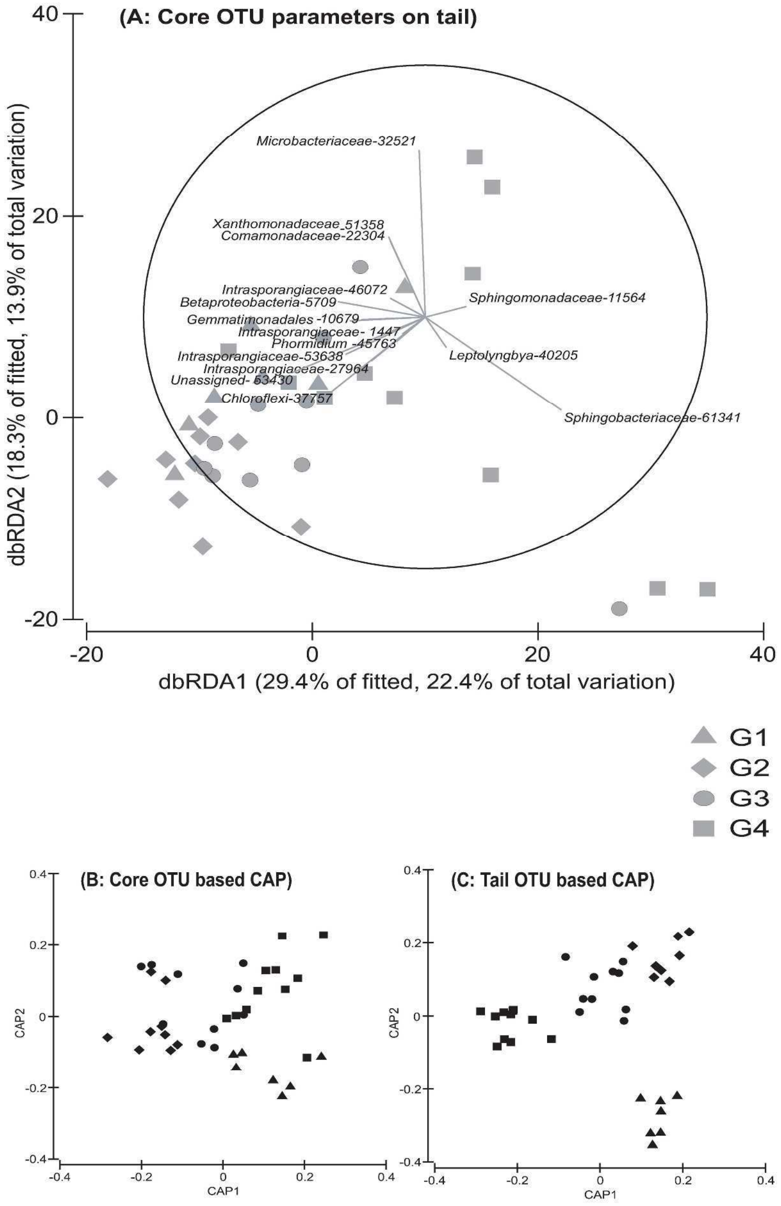

Distance-based redundancy analysis (dbRDA) ordination plot of distance-based linear models (A) of core predictors of tail community structure and Canonical Analysis of Principal Co-ordinates (CAP) of core and tail (panels B and C respectively) community structures according to sector.
244x379mm (300 x 300 DPI)

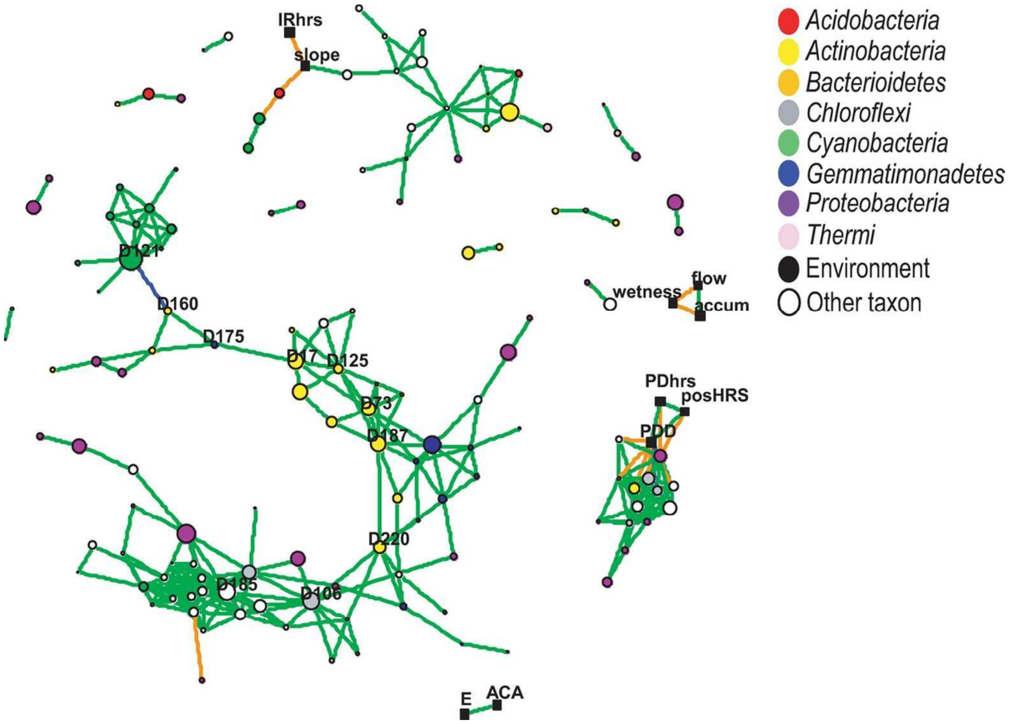

Community network based on significant pairwise Spearman correlations between OTUs (green – positive correlation, orange – negative correlation). Size of node is relative to average OTU abundance, while colour indicates OTU's phylum. Environmental variables have been included as nodes in the network and are indicated as black squares.
117x84mm (300 x 300 DPI)

Taxon interactions control the distributions of cryoconite bacteria colonizing a High Arctic ice cap

Jarishma K. Gokul, Andrew J. Hodson, Eli R. Saetnan, Tristram D.L., Irvine-Fynn, Philippa J. Westall, Andrew P. Detheridge, Nozomu Takeuchi, Jennifer Bussell Luis A.J. Mur, Arwyn Edwards.

SUPPLEMENTARY DATA:

Supplementary Figure 1: distance decay relationship between pairwise Bray Curtis distance between 16S sequencing profiles and pairwise physical distance.

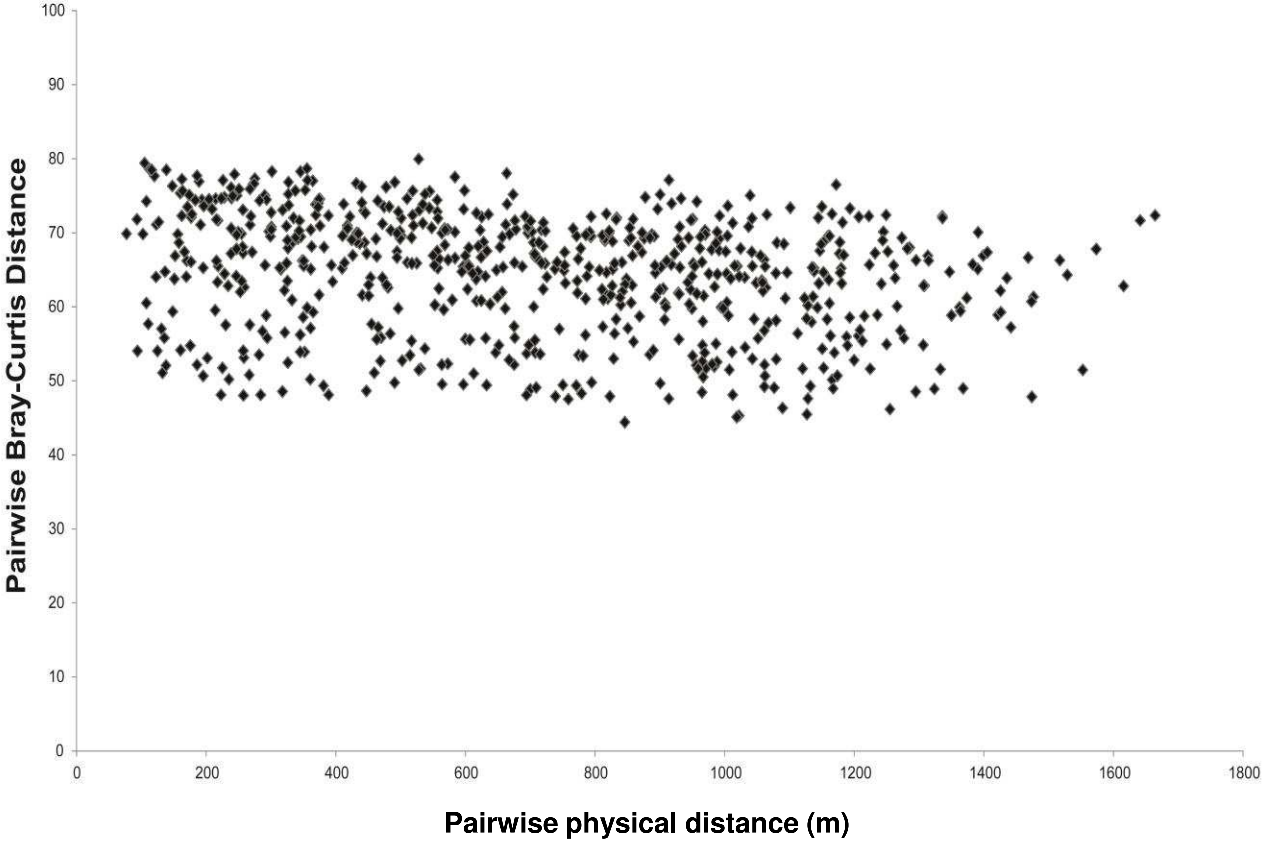

Supplementary Table 1. Modified primers used for amplification of bacterial 16S rRNA gene regions (5’-3’) V1-V3

Primer Name	**Forward primer (Primer A-key) (30)**	**Ion Barcode (10)**	**Spacer**	**Template specific sequence-3' (19)**	**Notes**
NGS_V1-V2_1	CCATCTCATCCCTGCGTGTCTCCGACTCAG	CTAAGGTAAC	GT	AGAGTTTGATCMTGGCTCAG	27F
NGS_V1-V2_2	CCATCTCATCCCTGCGTGTCTCCGACTCAG	TAAGGAGAAC	GT	AGAGTTTGATCMTGGCTCAG	
NGS_V1-V2_3	CCATCTCATCCCTGCGTGTCTCCGACTCAG	AAGAGGATTC	GT	AGAGTTTGATCMTGGCTCAG	
NGS_V1-V2_4	CCATCTCATCCCTGCGTGTCTCCGACTCAG	TACCAAGATC	GT	AGAGTTTGATCMTGGCTCAG	
NGS_V1-V2_5	CCATCTCATCCCTGCGTGTCTCCGACTCAG	CAGAAGGAAC	GT	AGAGTTTGATCMTGGCTCAG	
NGS_V1-V2_6	CCATCTCATCCCTGCGTGTCTCCGACTCAG	CTGCAAGTTC	GT	AGAGTTTGATCMTGGCTCAG	
NGS_V1-V2_7	CCATCTCATCCCTGCGTGTCTCCGACTCAG	TTCGTGATTC	GT	AGAGTTTGATCMTGGCTCAG	
NGS_V1-V2_8	CCATCTCATCCCTGCGTGTCTCCGACTCAG	TTCCGATAAC	GT	AGAGTTTGATCMTGGCTCAG	
NGS_V1-V2_9	CCATCTCATCCCTGCGTGTCTCCGACTCAG	TGAGCGGAAC	GT	AGAGTTTGATCMTGGCTCAG	
NGS_V1-V2_10	CCATCTCATCCCTGCGTGTCTCCGACTCAG	CTGACCGAAC	GT	AGAGTTTGATCMTGGCTCAG	
NGS_V1-V2_11	CCATCTCATCCCTGCGTGTCTCCGACTCAG	TCCTCGAATC	GT	AGAGTTTGATCMTGGCTCAG	
NGS_V1-V2_12	CCATCTCATCCCTGCGTGTCTCCGACTCAG	TAGGTGGTTC	GT	AGAGTTTGATCMTGGCTCAG	
NGS_V1-V2_13	CCATCTCATCCCTGCGTGTCTCCGACTCAG	TCTAACGGAC	GT	AGAGTTTGATCMTGGCTCAG	
NGS_V1-V2_14	CCATCTCATCCCTGCGTGTCTCCGACTCAG	TTGGAGTGTC	GT	AGAGTTTGATCMTGGCTCAG	
NGS_V1-V2_15	CCATCTCATCCCTGCGTGTCTCCGACTCAG	TCTAGAGGTC	GT	AGAGTTTGATCMTGGCTCAG	
NGS_V1-V2_16	CCATCTCATCCCTGCGTGTCTCCGACTCAG	TCTGGATGAC	GT	AGAGTTTGATCMTGGCTCAG	
NGS_V1-V2_17	CCATCTCATCCCTGCGTGTCTCCGACTCAG	TCTATTCGTC	GT	AGAGTTTGATCMTGGCTCAG	
NGS_V1-V2_18	CCATCTCATCCCTGCGTGTCTCCGACTCAG	AGGCAATTGC	GT	AGAGTTTGATCMTGGCTCAG	
NGS_V1-V2_19	CCATCTCATCCCTGCGTGTCTCCGACTCAG	TTAGTCGGAC	GT	AGAGTTTGATCMTGGCTCAG	
NGS_V1-V2_20	CCATCTCATCCCTGCGTGTCTCCGACTCAG	CAGATCCATC	GT	AGAGTTTGATCMTGGCTCAG	
NGS_V1-V2_21	CCATCTCATCCCTGCGTGTCTCCGACTCAG	TCGCAATTAC	GT	AGAGTTTGATCMTGGCTCAG	
NGS_V1-V2_22	CCATCTCATCCCTGCGTGTCTCCGACTCAG	TTCGAGACGC	GT	AGAGTTTGATCMTGGCTCAG	
NGS_V1-V2_23	CCATCTCATCCCTGCGTGTCTCCGACTCAG	TGCCACGAAC	GT	AGAGTTTGATCMTGGCTCAG	
NGS_V1-V2_24	CCATCTCATCCCTGCGTGTCTCCGACTCAG	AACCTCATTC	GT	AGAGTTTGATCMTGGCTCAG	
NGS_V1-V2_25	CCATCTCATCCCTGCGTGTCTCCGACTCAG	GATCTGCGAT	GT	AGAGTTTGATCMTGGCTCAG	
NGS_V1-V2_26	CCATCTCATCCCTGCGTGTCTCCGACTCAG	CAGCTCATCA	GT	AGAGTTTGATCMTGGCTCAG	
NGS_V1-V2_27	CCATCTCATCCCTGCGTGTCTCCGACTCAG	CAAACAACAG	GT	AGAGTTTGATCMTGGCTCAG	
NGS_V1-V2_28	CCATCTCATCCCTGCGTGTCTCCGACTCAG	GCAACACCAT	GT	AGAGTTTGATCMTGGCTCAG	
NGS_V1-V2_29	CCATCTCATCCCTGCGTGTCTCCGACTCAG	GCGATATATC	GT	AGAGTTTGATCMTGGCTCAG	
NGS_V1-V2_30	CCATCTCATCCCTGCGTGTCTCCGACTCAG	CGAGCAATCC	GT	AGAGTTTGATCMTGGCTCAG	
NGS_V1-V2_31	CCATCTCATCCCTGCGTGTCTCCGACTCAG	AGTCGTGCAC	GT	AGAGTTTGATCMTGGCTCAG	
NGS_V1-V2_32	CCATCTCATCCCTGCGTGTCTCCGACTCAG	GTATCTGCGC	GT	AGAGTTTGATCMTGGCTCAG	
NGS_V1-V2_33	CCATCTCATCCCTGCGTGTCTCCGACTCAG	CGAGGGCCCG	GT	AGAGTTTGATCMTGGCTCAG	
NGS_V1-V2_34	CCATCTCATCCCTGCGTGTCTCCGACTCAG	CAAATTCGGC	GT	AGAGTTTGATCMTGGCTCAG	
NGS_V1-V2_35	CCATCTCATCCCTGCGTGTCTCCGACTCAG	AGATTGACCA	GT	AGAGTTTGATCMTGGCTCAG	
NGS_V1-V2_36	CCATCTCATCCCTGCGTGTCTCCGACTCAG	AGTTACGAGC	GT	AGAGTTTGATCMTGGCTCAG	
NGS_V1-V2_37	CCATCTCATCCCTGCGTGTCTCCGACTCAG	GCATATGCAC	GT	AGAGTTTGATCMTGGCTCAG	
NGS_V1-V2_38	CCATCTCATCCCTGCGTGTCTCCGACTCAG	CAACTCCCGT	GT	AGAGTTTGATCMTGGCTCAG	
	Reverse primer (Primer P1-key) (23)				
PGM_V1-V2_Rev	CCTCTCTATGGGCAGTCGGTGAT			CTGCTGCCTYCCGTA	357R

Supplementary Table 2: Diversity indices and environmental parameters measured

Sample	Number of OTUs	Pielou's evenness (J')	Shannon H'(loge)	Eastings (UTM)	Northings (UTM)	Chlorophyll a µg/g	Z (masl)	SLOPE (deg)	ASPECT (deg, 0=N clockwise)	FAA (m^2)	FLOWLENGTH (m)	CURVATURE	WETNESS	PDDs (in summer)	PositiveHrs	PDHrs	IR (W)	IRh (hrs)	IRkW	ACA (%)
1.1	476	0.64	3.97	526316	8672566	6.69	700.66	11.46	242.41	5075.00	1349.65	-8.69	0.002	77	1544	4379.4	525700	1659.4	525.7	3.41
1.2	512	0.74	4.61	526293	8672774	5.16	713.43	9.84	248.24	525.00	108.28	0.02	0.019	77	1507	4263.2	523400	1716.8	523.4	1.86
1.3	517	0.72	4.53	526380	8673063	4.04	738.02	7.64	265.13	4225.00	840.00	0.05	0.002	77	1438	4050.0	518100	1793.2	518.1	5.51
1.4	517	0.79	4.96	526472	8673272	5.96	746.95	5.91	292.91	75.00	12.07	-4.54	0.079	77	1416	3976.3	512000	1834.9	512	21.71
1.5	519	0.73	4.57	526630	8673519	9.09	736.29	7.40	6.65	2175.00	552.19	0.22	0.003	77	1443	4064.5	495000	1846.0	495	5.48
1.6	487	0.70	4.30	526789	8673341	5.90	761.18	7.60	344.10	175.00	32.07	-1.66	0.043	77	1380	3862.6	496300	1845.3	496.3	5.53
1.7	515	0.75	4.68	526670	8673046	5.97	769.58	4.80	270.38	2650.00	525.00	-4.88	0.002	77	1354	3797.4	520800	1821.7	520.8	5.01
2.1	474	0.70	4.33	526733	8672710	11.86	765.80	5.97	235.00	875.00	240.42	-3.31	0.007	77	1366	3826.6	529400	1756.2	529.4	10.63
2.2	526	0.76	4.77	526835	8672646	10.71	770.32	5.18	225.56	2425.00	678.82	0.02	0.002	77	1351	3791.8	530900	1771.8	530.9	5.00
2.3	412	0.65	3.91	526895	8672534	8.18	766.07	5.09	212.24	625.00	169.71	-1.54	0.008	77	1366	3824.5	532600	1761.9	532.6	9.53
2.4	492	0.74	4.61	526972	8672534	7.70	769.90	3.90	200.16	100.00	15.00	1.03	0.039	77	1352	3795.0	531600	1769.7	531.6	6.54
2.5	550	0.76	4.79	527013	8672440	5.83	763.33	5.37	190.19	850.00	165.00	0.07	0.006	77	1372	3845.7	535500	1751.2	535.5	9.02
2.6	508	0.73	4.55	526890	8672376	9.62	753.78	6.12	213.92	325.00	80.71	0.09	0.019	77	1392	3921.2	533500	1747.3	533.5	10.75
2.7	543	0.72	4.54	526777	8672378	10.56	745.87	7.01	225.11	900.00	245.42	0.01	0.008	77	1416	3985.1	532000	1734.6	532	9.69
2.8	519	0.73	4.58	526668	8672418	5.41	738.35	8.88	227.49	1400.00	388.91	0.04	0.006	77	1437	4047.3	533200	1696.3	533.2	7.15
2.9	487	0.70	4.31	526877	8672788	5.57	781.12	4.12	240.82	1400.00	378.55	-3.37	0.003	77	1311	3711.5	527400	1796.2	527.4	2.24
3.1	470	0.72	4.44	527537	8672831	7.82	775.99	8.45	142.28	725.00	197.99	0.30	0.012	77	1329	3749.2	539000	1691.4	539	4.95
3.2	508	0.70	4.36	527486	8672736	9.19	768.83	9.67	137.37	775.00	212.13	-3.00	0.012	77	1359	3803.2	538700	1659.6	538.7	4.42
3.5	498	0.67	4.16	527045	8672191	13.11	742.79	4.51	175.76	2475.00	490.00	0.12	0.002	77	1424	4010.5	532200	1767.2	532.2	5.36
3.6	472	0.59	3.65	527145	8672345	15.39	753.08	6.43	152.94	150.00	35.36	0.12	0.043	77	1394	3926.8	535700	1736.2	535.7	3.54
3.7	508	0.72	4.50	527187	8672514	6.20	767.40	6.89	152.90	75.00	14.14	0.04	0.092	77	1364	3814.2	537700	1719.3	537.7	5.76
3.8	508	0.71	4.39	527280	8672675	6.68	778.96	6.57	150.39	200.00	49.50	0.21	0.033	77	1315	3727.3	537300	1737.7	537.3	3.43
3.9	363	0.67	3.95	527335	8672826	5.55	790.62	4.96	153.38	1250.00	259.50	-1.72	0.004	76	1292	3643.4	534900	1751.2	534.9	3.42
3.1	525	0.75	4.69	527320	8672919	1.99	798.06	4.80	166.87	175.00	30.00	-3.86	0.027	76	1275	3591.1	536300	1763.3	536.3	4.05
3.11	524	0.77	4.80	527145	8672780	4.11	790.61	3.70	193.78	600.00	115.00	0.20	0.006	76	1292	3643.5	532900	1785.5	532.9	2.30
3.12	551	0.77	4.86	527077	8672700	4.93	784.68	3.57	187.34	525.00	100.00	0.25	0.007	76	1302	3685.8	532400	1787.1	532.4	2.43
4.1	503	0.64	3.99	527629	8672814	6.92	760.11	12.83	135.50	1200.00	332.34	-4.79	0.011	77	1384	3871.0	541000	1505.6	541	7.32
4.2	501	0.76	4.72	527674	8673000	3.53	778.42	11.06	128.27	1000.00	275.77	-2.05	0.011	77	1318	3731.2	537100	1646.3	537.1	2.68
4.3	447	0.76	4.65	527628	8673164	4.80	798.04	7.08	116.10	50.00	7.07	0.17	0.142	76	1275	3591.2	530300	1764.2	530.3	10.76
4.4	399	0.72	4.31	527729	8673119	5.90	782.33	10.84	117.11	525.00	141.42	-1.05	0.021	76	1308	3702.8	531400	1676.6	531.4	19.32
4.5	396	0.69	4.10	527845	8673224	5.20	769.05	11.63	107.42	1025.00	200.00	0.16	0.011	77	1356	3801.5	524900	1690.6	524.9	31.57
4.6	458	0.76	4.65	527755	8673356	1.98	789.52	8.95	104.60	700.00	135.00	-6.10	0.013	76	1293	3651.2	525200	1744.9	525.2	24.69
4.7	329	0.68	3.92	527634	8673387	3.05	802.25	3.63	58.27	200.00	49.50	-2.69	0.018	74	1263	3562.3	518800	1843.9	518.8	15.37
4.8	432	0.69	4.19	527533	8673301	3.04	805.80	0.47	67.50	375.00	70.00	-4.49	0.001	74	1259	3538.1	526300	1845.3	526.3	13.11
4.9	353	0.67	3.94	527439	8672989	9.89	799.16	5.03	147.00	225.00	56.57	0.23	0.022	74	1266	3583.5	534900	1773.9	534.9	6.90
4.1	515	0.78	4.85	527518	8673083	6.74	801.15	4.54	138.50	500.00	134.35	-1.00	0.009	74	1263	3569.8	532800	1776.9	532.8	5.32
4.11	489	0.78	4.81	527679	8673259	2.51	796.90	7.16	106.71	300.00	55.00	-1.02	0.024	76	1278	3599.2	526700	1768.8	526.7	2.92

Supplementary Table 3: Pairwise PERMANOVA comparison of bacterial community structure (at the OTU level) by sector of Foxfonna ice cap

Groups	t	P(perm)
G1, G4	1.6398	0.004
G1, G2	1.7124	0.001
G1, G3	1.5446	0.003
G4, G2	2.2761	0.001
G4, G3	1.5973	0.003
G2, G3	1.4803	0.007

Supplementary Table 4: Marginal tests from distLM model of environmental predictors of bacterial community structure.

MARGINAL TESTS				
Variable	SS(trace)	Pseudo-F	P	Prop.
E	2351.7	3.8009	0.001	9.80E-02
N	2276.1	3.6659	0.001	9.48E-02
Chl a ug/g	1380.4	2.1353	0.012	5.75E-02
Z (masl)	1950.3	3.0947	0.002	8.12E-02
SLOPE (deg)	2217.8	3.5625	0.002	9.24E-02
ASPECT (deg, 0=N clockwise)	1861	2.9412	0.004	7.75E-02
ACCUMAREA (m^2)	705.35	1.0595	0.355	2.94E-02
FLOWLENGTH (m)	745.34	1.1214	0.283	3.10E-02
CURVATURE	623.13	0.93268	0.474	2.60E-02
WETNESS	538.76	0.80348	0.633	2.24E-02
PDDs (in summer)	3549	6.0717	0.001	0.14783
PositiveHrs	1915.8	3.0353	0.003	7.98E-02
PDHrs	1826.8	2.8827	0.003	7.61E-02
IR (W)	783.44	1.1807	0.238	3.26E-02
IRh (hrs)	1579.3	2.4646	0.003	6.58E-02
ACA (%)	1718.1	2.6979	0.012	7.16E-02

Supplementary Table 5: Sequential tests from distLM model of environmental predictors of bacterial community structure. SS: sums of squares; Pseudo-F: test statistic

Variable	Adj R^2	SS(trace)	Pseudo-F	P	Proportion explained	Cumulative variance
PDDs (in summer)	**0.12**	**3549.0**	**6.1**	**0.001**	**0.15**	**0.15**
SLOPE (deg)	**0.21**	**2588.5**	**4.9**	**0.001**	**0.11**	**0.26**
N	**0.24**	**1248.6**	**2.5**	**0.001**	**0.05**	**0.31**
ACA (%)	**0.27**	**1005.9**	**2.1**	**0.011**	**0.04**	**0.35**
E	**0.31**	**1372.8**	**3.0**	**0.002**	**0.06**	**0.41**
WETNESS	**0.31**	**503.5**	**1.1**	**0.319**	**0.02**	**0.43**
FAA (m^2)	**0.32**	**517.2**	**1.1**	**0.309**	**0.02**	**0.45**
IRkW	**0.32**	**459.1**	**1.0**	**0.399**	**0.02**	**0.47**
PDHrs	**0.33**	**661.2**	**1.5**	**0.106**	**0.03**	**0.50**
Z (masl)	**0.33**	**511.8**	**1.1**	**0.264**	**0.02**	**0.50**
IR (W)	**0.33**	**0.0**	**0.0**	**1.000**	**0.00**	**0.52**

Supplementary Table 6: BLAST matches of core OTUs to closest environmental relatives (CER) and closest named relatives (CNR)

Core OTU	CER	CER #	CER %id	CER Habitat	CNR	CNR #	CNR %id	CER Habitat
Sphingobacteriaceae-61341	Uncultured actinobacterium clone IC4008	HQ622724.1	99	Svalbard ice	Pedobacter daechungensis	NR_041507	89	Korean lake sediment
Microbacteriaceae-32521	Frigoribacterium sp. MP117	KC256951	99	Tibetan glacier	Frigoribacterium sp. MP117	KC256951	99	Tibetan glacier
Intrasporangiaceae-46072	Uncultured bacterium clone ANTLV2_G12	DQ521529	98	Lake Vida ice, Antarctica	Oryzihumus sp. aerobe-19	KP185144	93	Korean grassland
Chloroflexi-37757	Uncultured bacterium clone gls106	KC286738	98	Chinese glacier	Azospirillum sp. YM 195	GU396257.1	89	Sugarcane rhizome
Intrasporangiaceae-27964	Uncultured bacterium clone gs34	JF420640	97	German glacier sediment	Humibacter albus	AM494541	91	sewage sludge
Gemmatimonadales-59904	Uncultured bacterium clone NC54g8_19617	JQ377159	97	FACE soil	Ellin5220	AY234571	92	soil
Phormidium-45763	Uncultured cyanobacterium clone LJ14_522	KM112145	98	Antarctic microbial mat	Phormidium autumnale Ant-Ph68	DQ493874.1	98	Signy island, Antarctica
Leptolyngbya-40205	Uncultured bacterium clone IC4002	HQ622720	98	Svalbard ice	Phormidesmis priestleyi ANT.L66.	AY493581	95	Antarctica
Xanthomonadaceae-51358	Uncultured gamma proteobacterium clone TSC52	EU359963	98	Taiwanese soil	Pseudoxanthomonas sacheonensis	HF585486	94	US soil
Betaproteobacteria-10679	Uncultured bacterium isolate LH2-01	EU440469.1	98	Stromatolite, Canadian Arctic	Telluria mixta	LN794206	92	Germany
Intrasporangiaceae-53638	Uncultured bacterium clone LD_RB_26	EU644104	97	Siberian tundra	Ornithinimicrobium tianjinense	JQ948045	92	China
Betaproteobacteria-5709	Uncultured bacterium clone KuyT-ice-10	EU263777.1	97	Tibetan glacier	Massilia sp. 4106	JX566591.1	90	Chinese soil
Comamonadaceae-22304	Uncultured bacterium clone F35	FJ230911.1	98	Chinese river	Curvibacter	FN543107	98	Putative symbiont
Intrasporangiaceae-1447	Uncultured bacterium clone KuyT-IWPB-17	EU263719.1	99	Tibetan glacier	Eubacterium sp. 4c	AY216882	93	French peat
Sphingomonadaceae-11564	Uncultured bacterium clone GB7N87003GM6UD	HM728220	98	Antarctic soil	Novosphingobium sp. R1-11	KP182170	96	Korean soil
Unassigned-53430	Uncultured bacterium clone GB7N87003FR93L	HM732819.1	98	Antarctic soil	Rhizobium sp. AC86c1	AY776225.1	90	Ethiophian soil

Supplementary Table 7: Marginal tests from distLM model of core predictors of tail population structure

MARGINAL TESTS

Variable	SS(trace)	Pseudo-F	P	Prop.
Leptolyngbya-40205	2026	2.9744	0.005	7.83E-02
Microbacteriaceae-32521	3167.9	4.8847	0.001	0.12247
Betaproteobacteria-5709	4014	6.4291	0.001	0.15518
Gemmatimonadales-59904	3912.4	6.2373	0.001	0.15125
Chloroflexi-37757	4394.3	7.1628	0.001	0.16988
Unassigned-53430	4359.6	7.0947	0.001	0.16854
Sphingomonadaceae-11564	2592.8	3.8991	0.001	0.10024
Intrasporangiaceae-1447	2633.1	3.9666	0.002	0.1018
Intrasporangiaceae-46072	2889.7	4.4018	0.001	0.11172
Intrasporangiaceae-53638	3597.1	5.6533	0.001	0.13906
Intrasporangiaceae-27964	3161.2	4.873	0.001	0.12221
Betaproteobacteria-10679	2801	4.2502	0.001	0.10829
Phormidium-45763	1723.9	2.4991	0.007	6.66E-02
Xanthomonadaceae-51358	2411.6	3.5986	0.001	9.32E-02
Comamonadaceae-22304	2725	4.1213	0.001	0.10535
Sphingobacteriaceae-61341	4527.6	7.4262	0.001	0.17504

Supplementary Table 8: Sequential tests from distLM model of core predictors of tail population structure

Variable	Adj R^2	SS(trace)	Pseudo-F	P	Proportion explained	Cumulative variance
Sphingobacteriaceae-61341	0.15147	4527.6	7.4262	0.001	0.175	0.17504
Microbacteriaceae-32521	0.26094	3284	6.1843	0.001	0.127	0.302
Intrasporangiaceae-46072	0.34344	2487.1	5.2721	0.001	0.096	0.39815
Chloroflexi-37757	0.40126	1801.3	4.187	0.001	0.070	0.46779
Intrasporangiaceae-27964	0.44508	1406.3	3.53	0.001	0.054	0.52215
Gemmatimonadales-59904	0.48589	1278.4	3.46	0.001	0.049	0.57158
Phormidium-45763	0.50599	788.11	2.22	0.001	0.030	0.60205
Leptolyngbya-40205	0.52088	654.59	1.90	0.002	0.025	0.62735
Xanthomonadaceae-51358	0.5314	548.33	1.63	0.005	0.021	0.64855
Betaproteobacteria-10679	0.53992	495.83	1.50	0.024	0.019	0.66772
Intrasporangiaceae-53638	0.54681	454.44	1.40	0.058	0.018	0.68529
Betaproteobacteria-5709	0.55312	434.32	1.35	0.074	0.017	0.70208
Comamonadaceae-22304	0.55863	412.16	1.30	0.112	0.016	0.71801
Intrasporangiaceae-1447	0.56352	394.48	1.26	0.139	0.015	0.73326
Sphingomonadaceae-11564	0.5677	376.68	1.21	0.187	0.015	0.74783
Unassigned-53430	0.5711	359.44	1.17	0.255	0.014	0.76172

Supplementary Table 9: Marginal tests from distLM model of environmental and core OTU predictors of total population structure

Variable	SS(trace)	Pseudo-F	P	Prop.
E	2351.7	3.8009	0.001	9.80E-02
N	2276.1	3.6659	0.001	9.48E-02
Chl a ug/g	1380.4	2.1353	0.019	5.75E-02
Z (masl)	1950.3	3.0947	0.003	8.12E-02
SLOPE (deg)	2217.8	3.5625	0.001	9.24E-02
ASPECT (deg, 0=N clockwise)	1861	2.9412	0.005	7.75E-02
ACCUMAREA (m^2)	705.35	1.0595	0.329	2.94E-02
FLOWLENGTH (m)	745.34	1.1214	0.271	3.10E-02
CURVATURE	623.13	0.93268	0.47	2.60E-02
WETNESS	538.76	0.80348	0.633	2.24E-02
PDDs (in summer)	3549	6.0717	0.001	0.14783
PostitveHrs	1915.8	3.0353	0.003	7.98E-02
PDHrs	1826.8	2.8827	0.004	7.61E-02
IR (W)	783.44	1.1807	0.226	3.26E-02
IRh (hrs)	1579.3	2.4646	0.013	6.58E-02
IRkW	783.44	1.1807	0.258	3.26E-02
ACA (%)	1718.1	2.6979	0.01	7.16E-02
Leptolyngbya-40205	1725.2	2.7099	0.006	7.19E-02
Microbacteriaceae-32521	3062.2	5.1172	0.001	0.12756
Betaproteobacteria-5709	3148.9	5.2839	0.001	0.13117
Gemmatimonadales-59904	2730	4.4907	0.001	0.11372
Chloroflexi-37757	3180	5.344	0.001	0.13246
Unassigned-53430	2955.8	4.9144	0.001	0.12312
Sphingomonadaceae-11564	2736.5	4.5028	0.001	0.11399
Intrasporangiaceae-1447	1600.1	2.4993	0.014	6.67E-02
Intrasporangiaceae-46072	2090.7	3.3388	0.003	8.71E-02
Intrasporangiaceae-53638	2078.3	3.3172	0.005	8.66E-02
Intrasporangiaceae-27964	2223.5	3.5725	0.001	9.26E-02
Betaproteobacteria-10679	1582.9	2.4707	0.011	6.59E-02
Phormidium-45763	1317.8	2.0328	0.043	5.49E-02
Xanthomonadaceae-51358	1456.3	2.2602	0.009	6.07E-02
Comamonadaceae-22304	1625.1	2.5412	0.01	6.77E-02
Sphingobacteriaceae-61341	4713.8	8.5514	0.001	0.19635

Supplementary Table 10 : Sequential tests of environmental and core OTU predictors of total community structure

Variable	Adj R^2	SS(trace)	Pseudo-F	P	Proportion explained	Cumulative variance
Sphingobacteriaceae-61341	0.173	4713.8	8.55	0.001	0.2	0.2
Microbacteriaceae-32521	0.3	3431.6	7.36	0.001	0.14	0.34
Intrasporangiaceae-46072	0.377	2158.9	5.2	0.001	0.09	0.43
Intrasporangiaceae-27964	0.419	1298	3.35	0.001	0.05	0.48
Leptolyngbya-40205	0.454	1108.7	3.04	0.001	0.05	0.53
Chloroflexi-37757	0.476	815.45	2.33	0.001	0.03	0.56
Phormidium-45763	0.496	726.07	2.16	0.001	0.03	0.59
N	0.512	643.2	1.98	0.003	0.03	0.62
E	0.526	570.53	1.8	0.002	0.02	0.64
IRh (hrs)	0.535	473.19	1.53	0.018	0.02	0.66
Intrasporangiaceae -1447	0.543	447.6	1.47	0.05	0.02	0.68
Unassigned-53430	0.549	403.23	1.34	0.085	0.02	0.7
Betaproteobacteria-5709	0.555	384.11	1.29	0.137	0.02	0.72
PDHrs	0.563	426.21	1.46	0.045	0.02	0.73
Gemmatimonadales-59904	0.57	379.04	1.32	0.133	0.02	0.75
IR (W)	0.574	349.92	1.23	0.19	0.01	0.76
Xanthomonadaceae-51358	0.579	347.69	1.24	0.188	0.01	0.78
Betaproteobacteria-10679	0.585	344.71	1.24	0.227	0.01	0.79
PositiveHrs	0.588	319.18	1.16	0.308	0.01	0.81
Sphingomonadaceae-11564	0.59	291.21	1.07	0.405	0.01	0.82
PDDs (in summer)	0.599	306.95	1.15	0.296	0.01	0.86
Z (masl)	0.602	290.48	1.09	0.352	0.01	0.87
Sphingomonadaceae-11564	0.602	264.4	1	0.459	0.01	0.86

Supplementary Table 11: Sequential tests of environmental and core OTU predictors of tail community structure

Variable	Adj R^2	SS(trace)	Pseudo-F	P	Proportion explained	Cumulative variance
Sphingobacteriaceae-61341	0.17	4985.8	8.36	0.001	0.19	0.19
Microbacteriaceae-32521	0.292	3584.5	7.05	0.001	0.14	0.33
Intrasporangiaceae-46072	0.367	2287.7	5.03	0.001	0.09	0.42
Intrasporangiaceae-27964	0.408	1389.6	3.27	0.001	0.05	0.47
Leptolyngbya-40205	0.441	1172.5	2.92	0.001	0.05	0.52
Chloroflexi-37757	0.464	884.78	2.3	0.001	0.03	0.55
Phormidium-45763	0.483	791.69	2.13	0.001	0.03	0.58
N	0.5	700.72	1.95	0.002	0.03	0.61
E	0.513	623.48	1.78	0.005	0.02	0.63
Intrasporangiaceae-1447	0.523	526.4	1.53	0.022	0.02	0.66
IRh (hrs)	0.531	496.06	1.47	0.036	0.02	0.67
Unassigned-53430	0.537	441.15	1.33	0.09	0.02	0.69
PDHrs	0.542	414.92	1.26	0.168	0.02	0.71
Betaproteobacteria-5709	0.551	466.38	1.45	0.05	0.02	0.73
Gemmatimonadales-59904	0.556	408.67	1.28	0.165	0.02	0.74
IRkW	0.561	383.75	1.22	0.202	0.01	0.76
Xanthomonadaceae-51358	0.566	379.77	1.22	0.208	0.01	0.77
Z (masl)	0.571	379.05	1.23	0.208	0.01	0.79
Betaproteobacteria-10679	0.574	346.03	1.13	0.328	0.01	0.8
WETNESS	0.576	334.33	1.1	0.344	0.01	0.81
Sphingomonadaceae-11564	0.577	313.92	1.03	0.421	0.01	0.82
Intrasporangiaceae-53638	0.581	341.19	1.13	0.342	0.01	0.84
ACA (%)	0.582	312.92	1.04	0.443	0.01	0.85
PDDs (in summer)	0.587	344.06	1.16	0.324	0.01	0.86
CURVATURE	0.592	328.7	1.12	0.36	0.01	0.88
Chlorophyll a µg g^{-1}	0.592	296.43	1.01	0.45	0.01	0.89
PositiveHrs	0.593	298.39	1.02	0.438	0.01	0.9
Betaproteobacteria-5709	0.593	291.84	1	0.474	0.01	0.89

Supplementary Table 12: Marginal tests from distLM model of environmental and core OTU predictors of tail population structure

Variable	SS(trace)	Pseudo-F	P	Prop.
E	2472.3	3.6988	0.001	0.10
N	2445.5	3.65E+00	0.001	0.09
Chl a ug/g	1499.8	2.15E+00	0.021	0.06
Z (masl)	2101.1	3.09E+00	0.002	0.08
SLOPE (deg)	2369	3.53E+00	0.001	0.09
ASPECT (deg, 0=N clockwise)	1969.2	2.88E+00	0.001	0.08
ACCUMAREA (m^2)	769.03	1.07E+00	0.318	0.03
FLOWLENGTH (m)	812.22	1.13E+00	0.289	0.03
CURVATURE	668.69	9.29E-01	0.477	0.03
WETNESS	599.19	8.30E-01	0.59	0.02
PDDs (in summer)	3771.8	5.97E+00	0.001	0.15
PostitveHrs	2064.1	3.04E+00	0.002	0.08
PDHrs	1969.8	2.89E+00	0.003	0.08
IR (W)	825.09	1.15E+00	0.25	0.03
IRh (hrs)	1654.7	2.39E+00	0.008	0.06
IRkW	825.09	1.15E+00	0.275	0.03
Irhrs	1653.8	2.39E+00	0.013	0.06
ACA (%)	1802.4	2.62E+00	0.007	0.07
Leptolyngbya-40205	1809	2.6319	0.008	0.07
Microbacteriaceae-32521	3228	4.99E+00	0.001	0.12479
Betaproteobacteria-5709	3288	5.10E+00	0.001	0.12712
Gemmatimonadales-59904	2803.4	4.25E+00	0.001	0.10838
Chloroflexi-37757	3354	5.21E+00	0.001	0.12967
Unassigned-53430	3136.9	4.83E+00	0.001	0.12127
Sphingomonadaceae-11564	2850.5	4.33E+00	0.001	0.1102
Intrasporangiaceae-1447	1672.1	2.42E+00	0.019	6.46E-02
Intrasporangiaceae-46072	2197.4	3.25E+00	0.005	8.50E-02
Intrasporangiaceae-53638	2191.5	3.24E+00	0.006	8.47E-02
Intrasporangiaceae-27964	2328.9	3.46E+00	0.004	9.00E-02
Betaproteobacteria-10679	1639.1	2.368	0.016	6.34E-02
Phormidium-45763	1390.3	1.99E+00	0.042	5.38E-02
Xanthomonadaceae-51358	1559.1	2.2449	0.006	6.03E-02
Comamonadaceae-22304	1729.1	2.51E+00	0.007	6.68E-02
Sphingobacteriaceae-61341	4985.8	8.36E+00	0.001	0.19275